Computers and Chemical Engineering 174 (2023) 108246

Contents lists available at ScienceDirect

Computers and Chemical Engineering

journal homepage: www.elsevier.com/locate/compchemeng

# On the closed-loop stochastic dynamics of two-state nonlinear exothermic CSTRs with PI temperature control

Jesus Alvarez [a], Roberto Baratti [b,*]

[a] Universidad Autónoma Metropolitana, Departamento de Ingeniería de Procesos, 09340 México City, México
[b] Università degli Studi di Cagliari, Dipartimento di Ingegneria Meccanica, Chimica e Materiali, Cagliari I-9123, Italy

ARTICLE INFO

*Keywords:*
Close-loop stochastic reactor dynamics
PI control
Statistical process control
Fokker plank equation
Robust state PDF stability
In probability stability
Brownian state motion dynamics

ABSTRACT

Fokker-Planck (FP) partial differential equation (PDE) theory is applied to characterize the stochastic dynamics of a class of open-loop (OL) 2-state nonlinear exothermic continuous reactors with: (i) zero and time-varying mean noise disturbances, and (ii) linear proportional-integral (PI) temperature control. The characterization includes: (i) the stochastic on deterministic dynamics dependency, (ii) gain condition for robust probability density function (PDF) stability over deterministic-diffusion time biscale with stationary monomodality at prescribed most probable (MP) state, (iii) evolutions of along nearly deterministic time scale of MP state and control and their variabilities, (iv) attainment of random motion in-probability (IP) stability over deterministic-diffusion time biscale, and (v) identification of the compromise between MP state regulation speed, robustness, and control effort. The methodological developments and findings are illustrated with three indicative examples with OL complex (bimodal and vulcanoid) stationary state PDFs, including analytic assessment as well as state PDF and random motion numerical simulation.

## 1. Introduction

Closed-loop (CL) industrial exothermic continuous stirred tank reactors (CSTRs) with complex open-loop (OL) nonlinear (NL) dynamics and linear proportional-integral (PI) control operate in the presence of exogenous (inlet composition and temperature, heat exchange rates, actuator, and measurement, etc.) and endogenous (quasi-stationary dynamics, imperfect mixing-transport, etc.) parasitic (high frequency) fluctuations (Jazwinski, 1970; Risken, 1996; Gardiner, 1997). By complex deterministic dynamics it is meant with NL phenomena, that occur "in the large" (beyond locality) such as steady-state (SS) multiplicity and/or limit cycling (LC) (Hubbard and West, 1995). Safety, disturbance and/or fault detection, reliability, product quality assessments and set-point adjustment (Ratto, 1998; Ratto and Paladino, 2000) are executed in a supervisory layer (Burr, 1976; McAvoy, 2002), by ad hoc combinations of PI and statistical process (SP) control techniques. The development of more systematic means to combine PI and SP control for chemical units subjected to parasitic fluctuations is a relevant problem along current industrial trends (Samad, 2017; Maxim et al., 2019).

The OL stochastic stationary dynamics of the indicative 2-state reactor class addressed in the present study has been analyzed over 5 decades with local (per stable SS) Monte Carlo (MC) simulation, reporting that: (i) reasonable state mean and covariance results are obtained in away from deterministic bifurcation condition (Pell and Aris, 1969; Doraiswamy and Kulkarny, 1986; Ratto, 1998; Mandur and Budman, 2014), and (ii) the method breaks down (Pell and Aris, 1969; Ratto, 1998) or yields atypical results (Doraiswamy and Kulkarny, 1986) in close to deterministic bifurcation. Recently (Alvarez et al., 2018), the OL PDF dynamics has been characterized with Fokker Planck (FP) partial differential equation (PDE) theory (Risken, 1996), establishing that: (i) the state PDF motions robust (R) converge, over deterministic -probability diffusion time biscale (without metastability), towards a monomodal stationary state PDF and if and only if the deterministic global dynamics are R monostable, and (ii) when the stationary state PDF is not monomodal, there can be metastable state PDF evolutions (Risken, 1996; Gardiner, 1997), depending on the initial state PDF, and (iii) a metastable state PDF evolves along deterministic-diffusion-escape time triscale. It was explained why the MC method of previous reactor studies: (i) breaks down in close to deterministic bifurcation, and (ii) cannot describe the purely stochastic phenomena (inexistent in deterministic systems) of transient along diffusion-metastability time biscale.

The CL 3-state stochastic stationary dynamics of the above discussed

* Corresponding author.
*E-mail address:* roberto.baratti@unica.it (R. Baratti).

https://doi.org/10.1016/j.compchemeng.2023.108246
Received 2 December 2022; Received in revised form 11 March 2023; Accepted 24 March 2023
Available online 28 March 2023

2-state reactor class with linear PI control has been analyzed local FP theory and MC simulation (Ratto, 1998; Ratto and Paladino, 2000), with emphasis on control gain selection in the light of state mean and variability along SP control considerations. It has been reported that: (i) as in the OL case (Pell and Aris, 1969), the MC approach breaks down in close to deterministic bifurcation, and (ii) the overcoming of this obstacle for efficient gain tuning requires a global FP PDE approach (Ratto, 1998).

Recently, stochastic exothermic reactors have been stabilized about an OL unstable mean SS with: (i) linear proportional control tuned with a stochastic sensitivity-ellipsoidal confidence technique (Bashkirtseva, 2018; Bashkirtseva and Pisarchik, 2018), and (ii) random state motion in-probability (IP) stabilizing (Krstic and Deng, 1988; Annunziato et al., 2014) passive (Lu et al., 2022) and economic model predictive (Wu et al., 2018a,b) NL SF control. The multiscale nature of the transient response issue has not been regarded.

The preceding considerations motivate the scope and novelty of the present study on an open and longstanding problem (Ratto, 1998; Ratto and Paladino, 2000) in the light of SP control considerations along past and current industrial trends (Samad, 2017; Maxim et al., 2019): the formal characterization with FP theory of the CL 3-state PDF dynamics of an indicative class of 2-state exothermic continuous reactors with complex NL OL deterministic dynamics, industrial-type linear proportional-integral (PI) temperature control, as well as endogenous zero-mean and exogenous time-varying mean noise disturbances.

The stochastic dynamics characterization includes: (i) the derivation of a gain condition for robust (R) CL state PDF motion stability towards a monomodal stationary state PDF, without metastability, (ii) the assessment of state PDF transient over deterministic-diffusion time biscale, (iii) the identification of the compromise between MP state regulation speed, robustness, and control effort, (iv) the implication of state PDF stability on random state motion IP stability (Wu et al., 2018a,b; Lu et al., 2022), and (v) verification through FP PDE-based state PDF (Alvarez et al., 2018) and SDE-based random motion (Wu et al., 2018a, b; Lu et al., 2022) simulations of methodological developments and findings with indicative examples underlain by complex OL state PDF dynamics (with bimodal and vulcanoid stationary state PDF) (Alvarez et al., 2018).

The methodological point of the departure is the FP PDE-based state PDF modeling of OL 2-reactors with complex OL PDF dynamics (Alvarez et al., 2018), where the correspondence between CL state PDF monomodality and deterministic monostability was established with the analytic solution of the stationary 2-state FP PDE. With respect to this study, the solution of the above stated CL stochastic 3-state reactor stochastic modeling problem requires the overcoming of two technical difficulties: (i) the correspondence between CL stationary state PDF monomodality and deterministic monostability must be studied with a method that circumvents the difficult or infeasible task of analytically solving the CL 3-state stationary state PDF, and (ii) means to characterize MP state and control evolutions and their variabilities are lacking. These difficulties are overcome by combining notions and tools from: (i) FP PDE fluctuation-dissipation (Ao, 2004; Kwon et al., 2005; Wang et al., 2006) and functional analysis-based dynamics (Jazwinski, 1970; Markowich and Villani, 2000), and (ii) deterministic NL dynamics (La Salle and Lefschetz, 1961; Hirsch and Smale, 1974; Sontag, 2008) and control (Isidori, 1999). The proposed state PDF stability approach is put in perspective with the state IP stability approach (Krstic and Deng, 1988; Tsinias, 1998) employed in previous chemical reactors studies (Wu et al., 2018a,b; Lu et al., 2022).

The contents are organized as follows. In Section 2 the problem is technically stated. In Section 3, deterministic CL R monostability is characterized in terms of passivity and control gains. In Section 4, a gain condition for R state PDF stability with stationary PDF monomodality is derived, the open-to-closed state PDF spatiotemporal geometric change is assessed, and it is shown that state PDF stability implies state IP stability. In Section 5, the MP state and control and their covariance evolutions are characterized. In Section 6, the proposed approach is illustrated with three examples with OL complex (bimodal and vulcanoid) stationary state PDF geometries, including FP PDE and SDE simulation. In Section 7, conclusions are drawn. The acronyms employed are listed in Table 1.

## 2. Control problem

Consider the benchmark class of exothermic CSTRs modeled by the deterministic mass and heat balances in dimensionless form (Aris, 1965; Alvarez et al., 2018):

$$\dot{x}_1 = \theta(x_{1e} - x_1) - \delta r(x_1, x_2) := g_1(\boldsymbol{z}, \boldsymbol{d}),\ \boldsymbol{z}:\ (3b) \tag{1a}$$

$$\dot{x}_2 = \theta(x_{2e} - x_2) - \eta(x_2 - \bar{x}_{2c}) + (\delta/2) r(x_1, x_2) + \eta u := g_2(\boldsymbol{z}, \boldsymbol{d}, u) \tag{1b}$$

$$y = x_2,\quad x_1(0) = x_{1o},\quad x_2(0) = x_{2o} \tag{1c}$$

with nominal statics

$$\bar{\theta}(\bar{x}_{1e} - \bar{x}_1) - \delta r(\bar{x}_1,\ \bar{x}_2) = 0 \tag{2a}$$

$$\bar{\theta}(\bar{x}_{2e} - \bar{x}_2) - \eta(\bar{x}_2 - \bar{x}_{2c}) + (\delta/2) r(\bar{x}_1, \bar{x}_2) = 0 \tag{2b}$$

where

$$\begin{aligned} x_1 \quad &= \quad C/C_r,\ x_1 = T/T_r,\ u = x_{2c} - \bar{x}_{2c}\, C_r = \bar{C}_e,\ T_r = \bar{T}_e, T_a \\ &= (-\Delta_a) C_r / (\rho c_p T_r) = 1/2,\ \eta = UA / (\bar{Q} \rho c_p) >_r 0, \theta = Q / \bar{Q},\quad \dot{(\cdot)} \\ &= \frac{d(\cdot)}{dt},\ t = t_a / t_\theta,\quad t_\theta = V / \bar{Q}\delta = \bar{R}V/(\bar{Q}C_r,\ r(x_1,\ x_2) \\ &= R(C_r x_1,\ T_r x_2)/\bar{R},\ \bar{R} = R(\bar{C}, \bar{T}) \end{aligned}$$

In the ODE (1): $x_1$ (or $x_2$) is the concentration (or temperature) state, $x_{1e}$ (or $x_{2e}$) is the feed concentration (or temperature) input, $x_{2c}$ is the coolant temperature, $\delta$ (or $\eta$) is the Damköhler (or Stanton) dimensionless number, $r$ is the reaction rate function, $t_\theta$ (or $\theta$) is the dimensionless nominal residence time (or dilution rate), $y$ is the measured temperature, $u$ is the jacket temperature control in deviation form with respect to the setpoint $\bar{y}$ associated with the (possibly nonunique and unstable) stable steady-state (SS) concentration-temperature pair $(\bar{x}_1, \bar{x}_2)$ of the nominal statics (2).

**Table 1**
Acronyms.

| Acronym | Meaning |
|---|---|
| CL | closed-loop |
| CSTR | continuous stirred tank reactor |
| E | exponentially |
| EUB | exponentially ultimately bounded |
| IS | input-to-state |
| IP | in probability |
| LC | limit cycle |
| LS | limit set |
| MP | most probable |
| NL | nonlinear |
| ODE | ordinary differential equation |
| OF | output-feedback |
| OL | open-loop |
| P | practically |
| MC | Monte Carlo |
| PDE | partial differential equation |
| PDF | probability density function |
| PI | proportional-integral |
| R | robust |
| RM | robustly monomodally |
| SDE | stochastic differential equation |
| STD | standard deviation |
| SF | state feedback |
| SS | steady-state |
| SP | statistical process |
| ZD | zero-dynamics |

### 2.1. Open-loop (OL) deterministic dynamics

In vector form, the *deterministic nonlinear (NL) OL 2-state reactor dynamics* (1) are written as

$$\begin{array}{rcl} \dot{\boldsymbol{z}} & = & \boldsymbol{g}(\boldsymbol{z},\boldsymbol{d},u),\ \boldsymbol{z}(0)=\boldsymbol{z}_o, y=\boldsymbol{c}_z\boldsymbol{z} \\ t & \geq & 0,\ \boldsymbol{z}\in Z\subset\Re^2,\ \boldsymbol{d}\in D\subset\Re^2 \end{array} \tag{3a}$$

where

$$\boldsymbol{z}=(x_1,\ x_2)^T,\ \boldsymbol{g}=(g_1,g_2)^T, \boldsymbol{c}_z=(0,1),\quad g_1,g_2:\ (1a-b),\ \boldsymbol{d}=(\theta,x_{1e},x_{2e})^T \tag{3b}$$

$$Z=\left\{\boldsymbol{z}=(x_1,x_2)^T\in\Re^2 \middle| 0\leq x_1\leq x_1^+, x_2^-\leq x_2\leq x_2^+\right\} \tag{3c}$$

$$x_1^+=x_{1e}^+,\quad x_2^-=\frac{\bar{\theta}x_{2e}^-+\eta x_{2c}^-}{\bar{\theta}+\eta},\quad x_2^+=\frac{(\bar{\theta}x_{1e}^+/2)+\bar{\theta}x_{2e}^++\eta x_{2c}^+}{\bar{\theta}+\eta} \tag{3d}$$

$\boldsymbol{z}$ (or $\boldsymbol{d}$) is the *state* (or input disturbance) in the bounded set $Z$ (or $D$), $Z$ is the invariant state space (Alvarez et al., 2018), and $\boldsymbol{z}_o$ is the initial state. The corresponding *limit set* (LS) is

$$\Im_z=\mathscr{S}_z\cup\mathscr{L}_z \tag{4a}$$

where

$$\mathscr{S}_z=\{\bar{z}_1,\cdots,\bar{z}_{n_s\geq 1}\}\supset\mathscr{S}_z^s,\ \boldsymbol{g}(\bar{z}_i,\bar{\boldsymbol{d}},0)=0,\quad \bar{z}\in\mathscr{S}_z \tag{4b}$$

is the set of steady-states (SSs), and

$$\mathscr{L}_z=\left\{\bar{z}_1(t),\ldots,\bar{z}_{n_l}(t)\right\},\ \boldsymbol{g}[\bar{z}_i(t),\bar{\boldsymbol{d}},0]=\dot{z}_i(t) \tag{4c}$$

is the set of limit cycles (LCs), $\mathscr{S}_z^s$ is the set of stable SSs, and $\bar{z}$ is the prescribed SS.

When the reaction rate $r$ in (3) is 1st-order (linear) in concentration and NL (with Arrhenius dependency) in temperature, over its Damköhler-Stanton ($\delta$-$\eta$) parameter space the deterministic reactor (3) has regions of monostability, bistability and limit cycling, delimited by saddle-node and Hopf bifurcation (Aris, 1965; Uppal et al., 1974; Aris, 1999; Alvarez et al., 2018).

For given $[\boldsymbol{z}_o,(\boldsymbol{d},u)(t)]$, the OL NL ODE (3) has a unique solution *state* motion

$$\boldsymbol{z}(t)=\boldsymbol{\tau}_z[t,\boldsymbol{z}_o,(\boldsymbol{d},u)(t)] \tag{5a}$$

and *measured output signal*

$$y(t)=\boldsymbol{c}_z\{\boldsymbol{\tau}_z[t,\boldsymbol{z}_o,(\boldsymbol{d},u)(t)]\} \tag{5b}$$

When $(\boldsymbol{d},u)=(\bar{\boldsymbol{d}},0)$, and $\boldsymbol{z}_o$ is not a stable SS, $\boldsymbol{z}(t)$ reaches asymptotically, with characteristic time $t_z$, a SS $\bar{\boldsymbol{z}}$ or a LC $\bar{\boldsymbol{z}}(t)$ (Gavalas, 1968; Alvarez et al., 1991), i.e.,

$$(\boldsymbol{d},u)(t)=(\bar{\boldsymbol{d}},\bar{u}),\ \boldsymbol{z}_o\notin\mathscr{S}_z^s\Rightarrow\boldsymbol{z}(t)\overset{t_z}{\to}\bar{\boldsymbol{z}}\in\mathscr{S}_z or\ \bar{\boldsymbol{z}}(t)\in\mathscr{L}_z,\ t_z=1/\lambda_z \tag{6}$$

The deterministic nonlinear dynamics (3) are called (Hubbard and West, 1995; Alvarez et al., 2018): (i) simple if they have a unique robustly stable SS, and (ii) complex if they have multiplicity and/or limit cycling. Robustness means structural stability in the sense that small parameter deviations do not produce qualitative changes in the geometry of the global dynamics. Awayness from (or closeness to) bifurcation implies robustness (or fragility). Saddle-node and Hopf bifurcation are the mechanisms by which SSs and limit cycles are created or destroyed by parameter changes.

### 2.2. Open-loop (OL) stochastic dynamics

The effect in the deterministic dynamics (3) of endogenous parasitic fluctuations (temperature, and concentration variations, as well as reaction and mixing-transport quasi-SS assumptions) and of about mean fluctuations of the exogenous input (feed flow rate, inlet concentration, and temperature) disturbances is expressed as a zero-mean uncorrelated white noise concentration ($\xi_1$) and temperature ($\xi_2$) rate of change inputs, according to the stochastic differential equations (SDEs) (Pell and Aris, 1969; Doraiswamy and Kulkarni, 1986; Ratto, 1998; Alvarez et al., 2018; Wu et al., 2018a,b; Lu et al., 2022):

$$\begin{array}{rcl} \dot{z}_1 & = & g_1(z_1,z_2,\theta,x_{1e})+\xi_1(t),\ z_1(0)=z_{1o} \\ \xi_1(t) & = & \mathscr{W}(0,\mathscr{g}_1),\ g_1,g_2:\ (1a-b) \end{array} \tag{7a}$$

$$\begin{array}{rcl} \dot{z}_2 & = & g_2(z_1,z_2,\theta,x_{2e},u)+\xi_2(t),\ z_2(0)=z_{2o} \\ \xi_2(t) & = & \mathscr{W}(0,\mathscr{g}_2),\ y=z_2 \end{array} \tag{7b}$$

which in vector form are written as the [also called Langevin (Risken, 1996)] equation

$$\dot{\boldsymbol{z}}=\boldsymbol{g}(\boldsymbol{z},\boldsymbol{d},u)+\boldsymbol{\xi}(t),\ \boldsymbol{z}(0)=\boldsymbol{z}_o\sim\mathscr{R}[\varsigma_o(\boldsymbol{z})],\ y=\boldsymbol{c}_z(\boldsymbol{z}),\ \boldsymbol{z}\in\mathscr{Z}\supseteq Z \tag{8a}$$

where

$$\boldsymbol{\xi}(t)=\mathscr{W}[0,\boldsymbol{Q}],\ \boldsymbol{\xi}=(\xi_1,\xi_2)^T,\ \boldsymbol{Q}=\begin{bmatrix}\mathscr{g}_1 & 0\\ 0 & \mathscr{g}_2\end{bmatrix},\ \mathscr{g}_1,\mathscr{g}_2>0 \tag{8bd}$$

$$\begin{array}{l} \mathscr{Z}=\left\{\boldsymbol{z}\in\Re^2 \middle| 0\leq x_1\leq(1+\varepsilon_1)x_1^+,\quad (1-\varepsilon_2)x_2^-\leq x_2\leq(1+\varepsilon_2)x_2^+\right\} \\ x_1^+,x_2^-,x_2^+:\ (3d),\ \varepsilon_i\approx\dfrac{1}{3} \end{array} \tag{8e}$$

$$\boldsymbol{d}_s(t)=\mathscr{W}[\boldsymbol{d},\boldsymbol{Q}_d],\ \boldsymbol{d}_s(t)=\boldsymbol{d}(t)+\boldsymbol{w}_d \tag{8f}$$

$\boldsymbol{d}$ is the (possibly time-varying) mean value of the exogenous stochastic input disturbance $\boldsymbol{d}_s$, $\boldsymbol{z}_o$ is the initial random state $\boldsymbol{z}_o$ with probability density function (PDF) $\varsigma_o(z)$ over the probabilistic state space $\mathscr{Z}$ (Alvarez et al., 2018).

For given $[\varsigma_o,(\boldsymbol{d},u)(t),\boldsymbol{Q}]$, the SDE (8) has as unique solution a bivariate *state PDF motion* (Risken, 1996; Gardiner, 1997)

$$\varsigma(\boldsymbol{z},t)=\tau_\varsigma[t,\varsigma_o(\boldsymbol{z}),\boldsymbol{d}(t),u(t)],\ \varsigma(\boldsymbol{z},t)\geq 0 \tag{9}$$

that: (i) satisfies the 2-state dynamic FP PDE (10) [presented and discussed in (Alvarez et al., 2018)]

$$t>0,\ \boldsymbol{z}\in\mathscr{I}_{\mathscr{Z}}:\partial_t\varsigma=\nabla\cdot\left[\frac{1}{2}\boldsymbol{Q}\nabla\varsigma-\boldsymbol{g}(\boldsymbol{z},\boldsymbol{d})\varsigma\right] \tag{10a}$$

$$t=0,\ \boldsymbol{z}\in\mathscr{Z}:\varsigma(\boldsymbol{z},0)=\varsigma_o(\boldsymbol{z});\ \ t\geq 0:\int_{\mathscr{Z}}\varsigma(\boldsymbol{z},t)d\boldsymbol{z}=1 \tag{10bc}$$

$$t\geq 0,\ \boldsymbol{z}\in\mathscr{B}_{\mathscr{Z}}:\ \frac{1}{2}\boldsymbol{Q}\nabla\varsigma-\boldsymbol{g}(\boldsymbol{z},\boldsymbol{d})\varsigma=0 \tag{10d}$$

and (ii) when $(\boldsymbol{d},u)=(\bar{\boldsymbol{d}},0)$ and $\varsigma_o(\boldsymbol{z})\neq\bar{\varsigma}(\boldsymbol{z})$, $\varsigma(\boldsymbol{z},t)$ (9) reaches asymptotically (along time scale $t_\varsigma$ with deterministic, diffusion and escape time subscales), a (monomodal or non-monomodal) stationary state PDF

$$\bar{\varsigma}(\boldsymbol{z})\geq 0,\ \int_{\mathscr{Z}}\bar{\varsigma}(\boldsymbol{z})d\boldsymbol{z}=1,\ \boldsymbol{z}\in\mathscr{Z}\supseteq Z \tag{11a}$$

according to the expressions

$$\boldsymbol{d}=\bar{\boldsymbol{d}},\ u=0,\ \varsigma_o(\boldsymbol{z})\neq\bar{\varsigma}(\boldsymbol{z})\Rightarrow\varsigma(\boldsymbol{z},t)\overset{t_\varsigma}{\to}\bar{\varsigma}(\boldsymbol{z}) \tag{11b}$$

where

$$\begin{array}{rcl} t_\varsigma & \approx & \begin{cases} t_e^o\geq t_d^o \text{ if } \varsigma(\boldsymbol{z},t) \text{ is metastable} \\ t_d^o\geq t_z \text{ if } \varsigma(\boldsymbol{z},t) \text{ is not metasable} \end{cases} \\ t_d^o & \approx & 1/\min(\mathscr{g}_1,\mathscr{g}_2)>t_z,\quad t_z=1/\lambda_z \end{array} \tag{11c}$$

$$\mathscr{E}_z=\Im_z\ni\bar{\boldsymbol{z}},\quad \bar{y}=\boldsymbol{c}_z(\bar{\boldsymbol{z}}),\quad \Im_z:\ (4) \tag{11d}$$

$t_z$, $t_d^o$, and $t_e^o$ are the OL deterministic diffusion and escape time scales, respectively, $\mathscr{E}_z$ -equal to the deterministic LS (4)- is the *extremum set (ES)* of the OL stationary PDF $\bar{\varsigma}(z)$ (11a), and $\bar{z}$ is the OL (possibly a minimum or saddle) extremum point of interest, which determines the temperature setpoint $\bar{y}$ for the CL reactor SDE (15) with PI control that will be discussed in the next two subsections.

When the reaction rate $r$ in (3) is linear (or NL with Arrhenius dependency) in concentration (or temperature), over its Damköhler-Stanton ($\delta$-$\eta$) parameter space: the stationary state PDF $\bar{\varsigma}(z)$ (11a) has regions of monomodality, bimodality, and vulcanoid shape underlain by deterministic monostability, bistability and limit cycling, respectively (Alvarez et al., 2018).

The state PDF dynamics (10) are called (Alvarez et al., 2018): (i) *simple* if the stationary state PDF $\bar{\varsigma}(z)$ (11a) is R monomodal with mode at the prescribed deterministic SS $\bar{z}=_r \mathscr{E}_z$ (11d), and (ii) *complex* if $\bar{\varsigma}(z)$ is non-monomodal (e.g., bimodal or vulcanoid). Stationary state PDF *robustness (or fragility)* means *structural stability (or instability)* of the PDF limit set $\mathfrak{S}_z$ (4a) *with respect to* small parameter deviations.

### 2.3. Closed-loop stochastic differential equation (SDE)

Consider the industrial-type *deterministic linear PI control*

$$u = PI(y), \quad PI(y) := \bar{u} - k_p\left\{(y-\bar{y}) + \tau_I^{-1}\int_0^{\prime}[y(\prime)-\bar{y}]d\prime\right\} \tag{12a}$$

with proportional gain $k_p$, reset time $\tau_I$, integral gain $k_I$, set point

$$\bar{y} = \boldsymbol{c}_z\bar{\boldsymbol{z}} \in S_z \ni \boldsymbol{g}(\bar{z},\bar{\boldsymbol{d}}) = 0,\ \boldsymbol{g}:(1a-b) \tag{12b}$$

determined by the nominal target (possibly, neither unique nor maximum) extremum $\bar{z}$ (4) of the (possibly non-monomodal) bivariate OL state PDF (11a), and gain set

$$K = \left\{\boldsymbol{k}\in\Re^2\middle|0<k_p\le k_p^+,\ 0<k_I\le k_I^+\right\},\ \boldsymbol{k} = \left[k_p,k_I\right]^T,\ k_I = k_p\big/\tau_I \tag{12c}$$

In the presence of measurement (or actuator) zero-mean uncorrelated white noise error $w_y$ (or $\xi_u$) with variance $\gamma_y$ (or $\gamma_u$), the measurement ($y$) and control ($u$) become random variables, and the PI controller (12a) acquires the *random variable form*

$$u = PI\left(y+w_y\right)+\xi_u,\ \xi_u = \mathscr{W}(0,\gamma_u),\ w_y = \mathscr{W}\left(0,q_y\right) \tag{13ac}$$

The application of this control to the OL NL 2-state SDE (8) yields the *CL NL 3-state SDE*

$$\dot{x}_1 = f_1(x_1,x_2,\theta,x_{1e}) + w_1,\ x_1(0) = x_{1o} \tag{14a}$$

$$\dot{x}_2 = f_2\left(x_1,x_2,x_3,\theta,x_{2e},k_p\right) + w_2,\ x_2(0) = x_{2o} \tag{14b}$$

$$\dot{x}_3 = f_3(x_2,k_I) + w_3,\ x_3(0) = x_{3o} \tag{14c}$$

$$y = \boldsymbol{c}_y\boldsymbol{x} - k_p w_y,\ u = \boldsymbol{c}_u\boldsymbol{x} + w_u \tag{14d}$$

where

$$f_1(x_1,x_2,\theta,x_{1e}) = g_1(x_1,x_2,\theta,x_{1e}),\ f_3(x_2,k_I) = k_I(x_2-\bar{x}_2) \tag{14e}$$

$$f_2\left(x_1,x_2,x_3,\theta,x_{2e},k_p\right) = g_2(x_1,x_2,x_3,\theta,x_{2e}) - \eta\left[k_p(x_2-\bar{x}_2)+x_3\right] \tag{14f}$$

$$\boldsymbol{c}_y = (0\ 1\ 0),\quad \boldsymbol{c}_u = \eta\left[0\ k_p\ 1\right],\ g_1,g_2:\ (1a-b) \tag{14g}$$

$$\boldsymbol{w} = \begin{bmatrix} w_1 \\ w_2 \\ w_3 \end{bmatrix} = \mathscr{W}[0,\boldsymbol{Q}(\boldsymbol{k})],\ \boldsymbol{Q}(\boldsymbol{k}) = \begin{bmatrix} q_1 & 0 & 0 \\ 0 & q_2(k_p) & q_c(\boldsymbol{k}) \\ 0 & q_c(\boldsymbol{k}) & q_3(k_I) \end{bmatrix} \tag{14h}$$

$$q_1 = \gamma_1,\ q_2\left(k_p\right) = \gamma_2 + \eta^2\left(\gamma_u + k_p^2 q_y\right),\ q_3(k_I) = k_I^2 q_y,\ q_c(\boldsymbol{k}) = -\eta k_p k_I q_y \tag{14j}$$

and $\boldsymbol{w}$ is a zero-mean correlated white noise vector with covariance $3\times 3$ matrix $\boldsymbol{Q}$.

In compact vector form, the CL 3-state SDE (14) is written as

$$\dot{\boldsymbol{x}} = \boldsymbol{f}(\boldsymbol{x},\boldsymbol{d},\boldsymbol{k}) + \boldsymbol{w},\ \boldsymbol{x}_o = \mathscr{R}[\pi_o(\boldsymbol{x})] \tag{15a}$$

$$y = \boldsymbol{c}_y\boldsymbol{x}\ + w_y,\ u = \boldsymbol{c}_u\boldsymbol{x} + w_u,\ \boldsymbol{x}\in\mathscr{X},\ u\in\mathscr{U},\ \boldsymbol{k}\in K \tag{15b}$$

where

$$\boldsymbol{x} = [x_1\ x_2\ x_3]^T,\ \boldsymbol{f} = [f_1\ f_2\ f_3]^T,\quad \boldsymbol{w}:\ (14h),\quad \mathscr{X} = \mathscr{Z}\times\mathscr{I}\supseteq X,\quad \mathscr{Z}:(8e) \tag{15c}$$

$$\mathscr{I} = \left\{x_3\in\Re\middle|(1-\varepsilon_3)x_3^- \le x_3 \le (1+\varepsilon_2)x_3^+\right\},\ \varepsilon_3\approx 1/3 \tag{15d}$$

$$f_1,\ f_2,\ f_3:\ (14e-f),\ \boldsymbol{c}_y,\boldsymbol{c}_u:\ (14g),\quad K:\ (12c)$$

and $\mathscr{X}$ is the CL probabilistic state space. The SDE (15) has as solution the bundle of *Brownian random state motions* over $W$ (Kloeden and Platen, 1992; Risken, 1996; Gardiner, 1997)

$$\boldsymbol{x}(t) = \boldsymbol{\tau}_x^B[t,\boldsymbol{x}_o,\boldsymbol{d}(t),\boldsymbol{w}(t),\boldsymbol{k}],\ \boldsymbol{x}_o\in\mathscr{X}_o\subseteq\mathscr{X},\ \boldsymbol{w}(t)\in W,\ u = PI(\boldsymbol{c}_u\boldsymbol{x}+w_u) \tag{16}$$

The *CL SDE* (15) is said to be *in-probability (IP) stable* (Krstic and Deng, 1988, Wu et al., 2018a,b) if the probability

$$p(t,r) = P\{|\tilde{\boldsymbol{x}}(t)|\le r\},\ \tilde{\boldsymbol{x}}(t) = \boldsymbol{x}(t) - \bar{\boldsymbol{x}},\ \boldsymbol{f}(\bar{\boldsymbol{x}},\boldsymbol{d},\boldsymbol{k}) = 0 \tag{17a}$$

of having random motion deviations $\tilde{\boldsymbol{x}}(t)$ with bounded size $r$ is at least $1-\epsilon_p$, i.e.

$$p(t,r)\ge 1-\epsilon_p,\ 0\le\epsilon_p\le 1 \tag{17b}$$

### 2.4. Closed-loop probability density function (PDF) dynamics

According to stochastic calculus (Risken, 1996; Gardiner, 1997), for given $[\pi_o(\boldsymbol{x}),\boldsymbol{d}(t),\boldsymbol{Q}(\boldsymbol{k})]$, the complete information on the random state motion bundle (16) of the SDE (15) is contained in the unique *state PDF motion solution*

$$\pi(\boldsymbol{x},t) = \tau_\pi[t,\pi_o(\boldsymbol{x}),\boldsymbol{d}(t),\boldsymbol{k}],\ \pi(\boldsymbol{x},t)\ge 0 \tag{18}$$

of the 3-state dynamic FP PDE:

$$t>0,\ \boldsymbol{x}\in\mathscr{I}_{\mathscr{X}}:\ \partial_t\pi = \nabla\cdot\left[\frac{1}{2}\boldsymbol{Q}\nabla\pi - \boldsymbol{f}(\boldsymbol{x},\boldsymbol{d})\pi\right] := \mathscr{F}(\pi,\boldsymbol{d},\boldsymbol{k}) \tag{19a}$$

$$t=0,\ \boldsymbol{x}\in\mathscr{X}:\ \pi(\boldsymbol{x},0) = \pi_o(\boldsymbol{x});\ t\ge 0:\ \int_{\mathscr{X}}\pi(\boldsymbol{x},t)d\boldsymbol{x} = 1 \tag{19bc}$$

$$t\ge 0,\ \boldsymbol{x}\in\mathscr{B}_{\mathscr{X}}:\ \frac{1}{2}\boldsymbol{Q}\nabla\pi - \boldsymbol{f}(\boldsymbol{x},\boldsymbol{d})\pi := \boldsymbol{B}(\pi,\boldsymbol{d},\boldsymbol{k}) = 0 \tag{19d}$$

$$t\ge 0,\ u\in\mathscr{U}:\ \nu(u,t) = h[\pi(\boldsymbol{x},t)]\ge 0,\ u\in\mathscr{U}\int_{\mathscr{U}}\nu(u,t)du = 1 \tag{19e}$$

$$t\ge 0,\ \boldsymbol{x}\in\mathscr{X}:\ \boldsymbol{\psi} = \mathscr{Y}[\pi(\boldsymbol{x},t)] \tag{19f}$$

with initial (19b), conservation (19c) and boundary (19d) conditions. Here, $\mathscr{I}_{\mathscr{X}}$ (or $\mathscr{B}_{\mathscr{X}}$) is the interior (or boundary) of the probabilistic state space $\mathscr{X}$ (15c) and the output

$$\boldsymbol{\psi} = \{\boldsymbol{\psi}_1,\boldsymbol{\psi}_2\},\ \boldsymbol{\psi}_1 = \{\boldsymbol{x}_m,u_m,\Sigma_m,\sigma_u\} \tag{20a}$$

contains the PDF properties of interest in industrial SP control (Burr, 1976).

In the output $\boldsymbol{\psi}_1$ (20a) are included: (i) the state ($\boldsymbol{x}_m$) control ($u_m$) PDF modes (most probable -MP- values)

$$\boldsymbol{x}_m(t) = \arg\max_{\pi \in \mathscr{X}} \pi(\boldsymbol{x},t) := \boldsymbol{m}_x[\pi(\boldsymbol{x},t)],\ \nabla\pi(\boldsymbol{x}_m,t) = 0 \tag{20b}$$

$$u_m(t) = arg\max_{u \in \mathscr{U}} \nu(u,t) := m_u[\nu(u,t)],\quad \partial_u\nu(u_m,t) = 0 \tag{20c}$$

and (ii) the corresponding state ($\Sigma_m$) and control ($\sigma_u$) variabilities (co-variances)

$$\Sigma_m[\pi(\boldsymbol{x},t)] = \boldsymbol{H}^{-1}(\boldsymbol{x}_m,t),\ \sigma_u = \boldsymbol{v}_u(\mathrm{diag}\boldsymbol{\Sigma}_m)\boldsymbol{v}_u^T,\ \boldsymbol{v}_u = \left(0,\ k_p, 1\right) \tag{20d}$$

where

$$\boldsymbol{H}(\boldsymbol{x},t) = \mathscr{H}\pi(\boldsymbol{x},t),\quad \mathscr{H} = \nabla\nabla^T,\quad \nabla = \left(\partial_{x_1},\partial_{x_2},\partial_{x_3}\right)^T \tag{20e}$$

$$\nu(u,t) = \frac{1}{k_p}\int_{x_3^-}^{x_3^+} \mu_{x_2}\left[(u-x_3)/k_p\right]\mu_{x_3}(x_3,t)dx_3 \tag{20f}$$

$$\mu_{x_i}(x_i,t) = \int_{x_k^-}^{x_k^+}\int_{x_j^-}^{x_j^+} \pi(\boldsymbol{x},t)dx_j dx_k,\ i = 1,\ 2,\ 3,\ j,k \neq i \tag{20g}$$

$\nabla$ (or $\boldsymbol{H}$) is the gradient vector (or matrix Hessian) operator, (20e) determines the 1D control PDF $\nu$ from the 3D state one $\pi$ (Papoulis and Pillai, 2002), and $\mu_{x_i}$ is the marginal PDF with respect to the state $x_i$ (Papoulis and Pillai, 2002). In the output $\boldsymbol{\psi}_2$ (20a) can be included other properties such as state and control mean and their variabilities, the probability of having a within-range random state (17) (Wu et al., 2018a,b), and skewness measures like kurtocity.

When $\boldsymbol{d} = \bar{\boldsymbol{d}}$ and $\pi_o(\boldsymbol{x}) \neq \bar{\pi}(\boldsymbol{x})$, the PDF motion state motion $\pi(\boldsymbol{x},t)$ (18) and control evolution $\nu(u,t)$ (20f) reach asymptotically (along time scale $t_\pi$) the stationary PDFs $\bar{\pi}(\boldsymbol{x})$ and $\bar{\nu}(u)$, i.e.,

$$\boldsymbol{d} = \bar{\boldsymbol{d}},\ \pi_o(\boldsymbol{x}) \neq \bar{\pi}(\boldsymbol{x}) \Rightarrow \pi(\boldsymbol{x},t) \overset{t_\pi}{\to} \bar{\pi}(\boldsymbol{x}),\ \nu(u,t) \overset{t_\pi}{\to} \bar{\nu}(u),\ \boldsymbol{\psi} \overset{t_\pi}{\to} \bar{\boldsymbol{\psi}}(u) \tag{21a}$$

where

$$\begin{aligned} t_\pi(\boldsymbol{k}) &\approx \begin{cases} t_e \geq t_d \text{ if } \quad \pi(\boldsymbol{x},t) \text{ is metastable} \\ t_d \geq t_x \text{ if } \ \pi(\boldsymbol{x},t) \text{ is not metastable} \end{cases} \\ t_d &\approx 1/\min(q_1,q_2,q_3)\rangle t_x = 1/\lambda_x \end{aligned} \tag{21b}$$

$t_x$, $t_d$, and $t_e$ are the CL deterministic, diffusion, and escape time scales, respectively, with stationary state PDF

$$\bar{\pi}(\boldsymbol{x}) \geq 0,\ \int_{\mathscr{X}} \bar{\pi}(\boldsymbol{x})d\boldsymbol{x} = 1;\ \bar{\nu}(u) \geq 0,\ \int_{\mathscr{U}} \bar{\nu}(u)du = 1 \tag{22}$$

The stationary state PDF (22): (i) uniquely satisfies the static FP PDE

$$\boldsymbol{x} \in \mathscr{I}_{\mathscr{X}}:\ \mathscr{F}(\bar{\pi},\bar{\boldsymbol{d}}) = 0,\ \int_{\mathscr{X}} \pi(\bar{\pi})d\boldsymbol{x} = 1 \tag{23a}$$

$$\boldsymbol{x} \in \mathscr{B}_{\mathscr{X}}:\ \boldsymbol{B}(\bar{\pi},\bar{\boldsymbol{d}}) = 0 \tag{23b}$$

$$u \in \mathscr{U}:\ \bar{\nu} = h(\bar{\pi}) \geq 0,\ u \in \mathscr{U},\ \int_{\mathscr{U}} \nu(u)du = 1 \tag{23c}$$

$$\boldsymbol{x} \in \mathscr{X}:\ \bar{\boldsymbol{\psi}} = \mathscr{Y}(\bar{\pi}) \tag{23d}$$

and (ii) has the extremum set (ES)

$$\mathscr{E} = \mathscr{P} \cup \mathscr{O}, \mathscr{P} = \left\{\boldsymbol{x}_1,\ldots,\boldsymbol{x}_{n_p\geq 1}\right\},\ \nabla\bar{\pi}(\boldsymbol{x}_i,\boldsymbol{k}) = 0 \tag{24a}$$

where

$$\mathscr{P} = \left\{\boldsymbol{x}_1,\ldots,\boldsymbol{x}_{n_p\geq 1}\right\},\ \nabla\bar{\pi}(\boldsymbol{x}_i,\boldsymbol{k}) = 0 \tag{24b}$$

is the set of extremum points $\boldsymbol{x}_i$, and

$$\mathscr{O} = \{\mathscr{O}_1,\cdots,\mathscr{O}_{n_c\geq 0}\},\ \mathscr{O}_i = \{\boldsymbol{x} \in \mathscr{X} | [\nabla\bar{\pi}(\boldsymbol{x})]\cdot\boldsymbol{n}_i(\boldsymbol{x})\} = 0, \underset{\bar{\boldsymbol{x}}_m}{=\boldsymbol{m}_x(\bar{\pi}),\ \boldsymbol{m}_x} : (20b) \tag{24c}$$

is the set of extremum curves $\mathscr{O}_i$ with normal unit vector $\boldsymbol{n}_i(\boldsymbol{x})$.

The *CL dynamic FP PDE* (19) is said to be *robustly monomodally (RM) stable* if: (i) CL dynamic FP PDE (19) has a R unique stationary state PDF $\bar{\pi}(\boldsymbol{x})$ (22) that is R monomodal with MP state $\bar{\boldsymbol{x}}_m$ (24c) at prescribed value $\bar{\boldsymbol{x}}$ determined by the nominal (possibly a minimum or saddle) extremum point $\bar{\boldsymbol{z}}$ (11d) of the OL (monomodal or non-monomodal) stationary state PDF $\bar{\varsigma}(z)$, (ii) the state PDF motions $\pi(\boldsymbol{x},t)$ (18) evolve, without metastability (21b) [ruled out by stationary PDF monomodality (Risken, 1996; Alvarez et al., 2018)], over deterministic-diffusion time biscale $(t_x,t_d)$ (21b), and (ii) the state PDF motion deviations $\widetilde{\pi}(\boldsymbol{x},t)$ (25c) (with respect to stationary PDF $\bar{\pi}$) are input-to-state (Sontag, 2008) exponentially ultimately bounded (EUB) as (Markowich and Villani, 2000; Frank, 2006)

$$|\widetilde{\pi}(\boldsymbol{x},t)|_H \leq a_\pi e^{-\lambda_\pi t}|\widetilde{\pi}_o|_H^+ + b_\pi|\widetilde{\boldsymbol{d}}|^+ \leq |\widetilde{\pi}|_H^+,\quad a_\pi,b_\pi,\lambda_\pi > 0 \tag{25a}$$

where

$$\boldsymbol{k} \in \mathscr{K}_m = \{\boldsymbol{k} \in K | \mathscr{E} =_r \bar{\boldsymbol{x}}_m = \bar{\boldsymbol{x}}\},\ \bar{\boldsymbol{x}} = \left(\bar{\boldsymbol{z}}^T,0\right)^T, \bar{\boldsymbol{z}} \in \mathscr{E}_z,\ \mathscr{E}: (24a),\ \mathscr{E}_z : (11d)\ \boldsymbol{c}_z(\bar{\boldsymbol{z}}) = \bar{y} \tag{25b}$$

$$\widetilde{\pi}(\boldsymbol{x},t) = \pi(\boldsymbol{x},t) - \bar{\pi}(\boldsymbol{x}),\ \widetilde{\pi}_o = \pi_o(\boldsymbol{x}) - \bar{\pi}(\boldsymbol{x}),\ |\widetilde{\pi}_o|_H^+ \leq |\widetilde{\pi}_o|_H^+,\ |\widetilde{\boldsymbol{d}}(t)| \leq |\widetilde{\boldsymbol{d}}|^+ \tag{25c}$$

$$|\widetilde{\pi}|_H^+ = a_\pi|\widetilde{\pi}_o|_H^+ + b_\pi|\widetilde{\boldsymbol{d}}|^+,\ b_\pi = (a_\pi/\lambda_\pi)l_{\boldsymbol{d}}^{\mathscr{F}},\ \lambda_\pi \approx 1/t_d,\ t_d \geq t_x,\quad t_d : (21b) \tag{25d}$$

$$|\mathscr{F}(\pi,\boldsymbol{d}) - \mathscr{F}(\bar{\pi},\bar{\boldsymbol{d}})| \leq l_\pi^{\mathscr{F}}|\boldsymbol{x}-\bar{\boldsymbol{x}}| + l_{\boldsymbol{d}}^{\mathscr{F}}|\widetilde{\boldsymbol{d}}|,\ \widetilde{\boldsymbol{d}} = \boldsymbol{d} - \bar{\boldsymbol{d}} \tag{25e}$$

$\widetilde{\boldsymbol{d}}$ is the deterministic input deviation, $|\ |$ (or $|\ |_H$) is the Euclidian vector (or Hilbert function) norm, $l_{\boldsymbol{d}}^{\mathscr{F}}$ is the Lipschitz constant of $\mathscr{F}$ with respect to $\boldsymbol{d}$, and $\mathscr{K}_m$ is the set of control gains where the CL FP PDE (19) is RM stable.

If admissible size ($|\widetilde{\pi}_o|_H^+$ and $|\widetilde{\boldsymbol{d}}|^+$) deviations produce admissible PDE motion deviations ($\widetilde{\pi}$) with admissible size ($|\widetilde{\pi}|_H^+$), the CL FP PDE (19) is said to be practically (P) stable (La Salle and Lefschetz, 1961). The handling with functional analysis of R state profile stability [a variant of state PDF RM stability (25)] can be seen in previous studies on an indicative CL deterministic tubular reactor with advanced NL (Franco de los Reyes et al., 2020) and saturated linear PI control (Franco de los Reyes and Alvarez, 2022) control.

### 2.5. Problem

Our problem and contribution consist in characterizing, on the basis of the FP PDE (19) and as improvement of the ones presented in Ratto's pioneering study (Ratto, 1998) in the light of SP control considerations along past and current industrial trends (Samad, 2017; Maxim et al., 2019), the CL 3-state PDF dynamics (18) of an indicative class (15) of stochastic 2-state exothermic continuous reactors with: (i) complex NL OL deterministic dynamics (3), (ii) industrial-type linear PI temperature control (12), (iii) zero-mean random noise, and (iv) exogenous random time-varying mean disturbance.

Specifically, we are interested in: (i) the control gain choice (25b) that ensures the RM stability (25) CL stochastic state PDF dynamics (18), (ii) the assessment of the CL state PDF transient (18) over deterministic-

diffusion time biscale $(t_x, t_d)$ (21b), (iii) the identification of the compromise between MP state (20b) regulation speed and variability (20a), robustness, and control effort in a suitable stochastic sense, (iii) the nature of the complex-to-simple geometric state PDF change in the open-to-closed passage, (iv) the identification of the stochastic role played by the proportional and integral control components (13), and (v) in putting state PDF RM stability (25) in perspective with random state IP stability (17) (Wu et al., 2018a,b; Lu et al., 2022).

The methodological problem is solved by combining notions and tools from: (i) the stochastic fluctuation-dissipation relationship associated to the FP PDE (Ao, 2004; Kwon et al., 2005; Wang et al., 2006), (ii) state PDF dynamics and stability (Jazwinski, 1970, Markowich and Villani, 2000; Frank, 2006), (iii) random state IP stability (Krstic and Deng, 1988; Tsinias, 1998; Wu et al, 2018a,b; Lu et al., 2022), (iv) deterministic NL dynamics (La Salle and Lefschetz, 1961; Hirsch and Smale, 1974; Hubbard and West, 1995; Sontag, 2008), and (v) deterministic passive control (Hirschorn, 1979; Isidori, 1999; Khalil, 2002; Sontag, 2008).

While in our previous OL 2-state reactor class (8) study (Alvarez et al., 2018) the correspondence between stationary state PDF monomodality and deterministic monostability was established with the analytic solution for the stationary state PDF (22) of the 2D FP PDE (11), here the same correspondence for the 3-state CL stochastic reactor (15) is obtained without having to solve analytically the 3D FP PDE (19).

To simply the notation, the explicit dependencies of vector, matrices, and operators on the gain $\boldsymbol{k}$ will be omitted and written explicity when convenient.

## 3. Closed-loop deterministic dynamics

As a fundamental ingredient for the CL stochastic dynamics assessment problem at hand, here the deterministic CL dynamics are characterized.

The elimination of noise in the SDE (15) yields the CL deterministic dynamics

$$\dot{\boldsymbol{x}} = \boldsymbol{f}(\boldsymbol{x}, \boldsymbol{d}),\ \boldsymbol{x}(0) = \boldsymbol{x}_o,\ \boldsymbol{x} \in X,\ \boldsymbol{f}:\ (14e-f) \tag{26a}$$

$$y = \boldsymbol{c}_y \boldsymbol{x},\ u = \boldsymbol{c}_u(\boldsymbol{x}),\quad u \in U,\quad \boldsymbol{c}_y, \boldsymbol{c}_u:\ (14g),\quad \boldsymbol{k} \in K:\ (12c) \tag{26b}$$

with:

(i) compact invariant set

$$X = Z \times I,\quad Z:\ (3c),\quad I = x_3 \in \Re\ |\left(x_3^- \le x_3 \le x_3^+\right) \tag{26c}$$

(ii) statics

$$\boldsymbol{f}(\bar{\boldsymbol{x}}, \bar{\boldsymbol{d}}) = 0,\ \bar{y} = \boldsymbol{c}_y \bar{\boldsymbol{x}} = \boldsymbol{c}_z \bar{\boldsymbol{z}} \in S_z,\ \bar{u} = 0 \tag{27}$$

(iii) state motion

$$\boldsymbol{x}(t) = \tau_{\boldsymbol{x}}[t, \boldsymbol{x}_o, \boldsymbol{d}(t)],\ y(t) = \boldsymbol{c}_y\{\tau_{\boldsymbol{x}}[t, \boldsymbol{x}_o, \boldsymbol{d}(t)]\} \tag{28}$$

and (iv) limit set

$$\mathfrak{S}_x = \mathscr{S}_x \cup \mathscr{L}_x \tag{29a}$$

where

$$\mathscr{S}_x = \{\bar{\boldsymbol{x}}_1, \ldots, \bar{\boldsymbol{x}}_{n_s \ge 1}\} \ni \bar{\boldsymbol{x}},\ \boldsymbol{f}(\bar{\boldsymbol{x}}_i, \bar{\boldsymbol{d}}) = 0,\ \bar{\boldsymbol{x}} = \left(\bar{\boldsymbol{z}}^T, \bar{x}_3\right)^T,\ \bar{x}_3 = 0,\ \bar{\boldsymbol{z}}:(4b) \tag{29b}$$

is the set of SS points $\bar{\boldsymbol{x}}_1$, and

$$\mathscr{L}_x = \left\{O_1(t), \ldots, O_{n_l}(t)\right\},\ \boldsymbol{f}[\bar{\boldsymbol{x}}_i(t), \bar{\boldsymbol{d}}] = \dot{\boldsymbol{z}}_i(t), O_i = \left\{\boldsymbol{x} \in X \middle| \boldsymbol{x} = \bar{\boldsymbol{x}}_i(t), 0 \le t \le t_i^x\right\} \tag{29c}$$

is the set of SS limit cycles (LCs) points $\bar{\boldsymbol{x}}_i(t)$.

### 3.1. Passivity

Following the NL SF control approach (Isidori, 1999; Sepulchre et al., 2012) for chemical reactors (Alvarez et al., 1991), the enforcement of the setpoint $(\bar{y})$-based isothermal operation conditions

$$x_2 = \bar{y} = \bar{x}_2,\ \dot{x}_2 = 0 \tag{30}$$

on the OL deterministic reactor (3) yields the 1-dimensional dynamical inverse (Hirschorn, 1979)

$$\dot{x}_1 = g_z(x_1, \bar{y}, \theta, x_{1e}),\ x_1(0) = x_{1o};\ u = \mu_z(x_1, \theta, x_{2e}),\ x_1 \in X_1 = \left[0, \bar{x}_{1e}^+\right] \tag{31ab}$$

where

$$g_z(x_1,\ \bar{y}, \theta, x_{1e}) = \theta(x_{1e} - x_1) - \delta r(x_1, \bar{y}),\ g_z(\bar{x}_1, \bar{y}, \bar{\theta}, \bar{x}_{1e}) = 0 \tag{31cd}$$

$$\mu_z(x_1, \theta, x_{2e}) = -\frac{1}{\eta}[\theta(x_{2e} - \bar{y}) - \eta(\bar{y} - \bar{x}_{2c}) + (\delta/2) r(x_1, \bar{y})],\quad \eta \neq_r 0 \tag{31ef}$$

(31a) is the isothermal (at temperature $x_2 = \bar{y}$) concentration zero (output deviation) (ZD) dynamics (1a), (31b) is the output map that adjusts the control $u$ to keep the temperature fixed at $\bar{x}_2$, and $\eta \neq_r 0$ is the associated relative degree equal to one (RD = 1) condition. The OL reactor (3) is passive if: (i) it has RD = 1 (31e), and (ii) its ZD (31a) are R $\bar{x}_1$-monostable.

The RD = 1 condition is met with a sufficiently large Stanton number $\eta >_r 0$. The ZD (31a) are R $\bar{x}_1$-monostable if and only if the map $g_z$ (31c): (i) is R $x_1$-antitonic over $X_1$, i.e.,

$$\partial_{x_1} f_1(x_1, \bar{y}, \theta, x_{1e}) = -\theta - \partial_{x_1} r(x_1, \bar{y}) <_r 0\ \forall\ x_1 \in\ X_1 \tag{32a}$$

and (ii) with $(\bar{\theta}, \bar{x}_{1e})$, it vanishes at the nominal concentration value $\bar{x}_1$, i.e.,

$$g_z(\bar{x}_1, \bar{y}, \bar{\theta}, \bar{x}_{1e}) = 0 \tag{32b}$$

This passivity characterization is summarized in the next proposition.

**Proposition 1.** The deterministic OL system (3) is R passive if and only if ($>_r$: *"sufficiently larger than"*)

$$(i)\ \eta \neq_r 0,\ (ii)\ \bar{\theta} + \partial_{x_1} r(x_1, \bar{y}) >_r 0\ \forall\ x_1 \in X_1 \tag{33ab}$$

The passivity property (33) (Isidori, 1999; Sepulchre et al., 2012) of the reactor class (Alvarez et al., 1991): (i) is the solvability condition for the NL R stabilizing SF control problem, and (ii) delimits the attainable CL behavior with any SF control.

### 3.2. Steady-state (SS) uniqueness and local stability

In detailed form, the CL deterministic statics (27) (with $\boldsymbol{d} = \bar{\boldsymbol{d}}$) are written as

$$\bar{\theta}(\bar{x}_{1e} - x_1) - \delta r(x_1, x_2) = 0 \tag{34a}$$

$$\bar{\theta}(\bar{x}_{2e} - \bar{x}_2) - \eta\left[x_2 - \bar{x}_{2c} + k_p(x_2 - \bar{y}) + x_3\right] + (\delta/2) r(x_1, x_2) = 0 \tag{34b}$$

$$k_I(x_2 - \bar{y}) = 0,\quad \bar{y} = \bar{x}_2 \tag{34c}$$

The unique-trivial solution for temperature $x_2$ of the integral action

Eq. (34c) is (35a), the passivity property (33b) ensures the unique solution (35b) for concentration $x_1$ of the static mass balance (34a), and the substitution of (34a) in (34b) followed by the unique solution (35c) for $x_3$:

$$x_2 = \bar{y} = \bar{x}_2,\ x_1 = m(\bar{y}) := \bar{x}_1,\ x_3 = h(\bar{y}) = 0 := \bar{x}_3 \tag{35ac}$$

where

$$x_1 = m(\bar{y}) \Leftrightarrow \bar{\theta}(\bar{x}_{1e} - x_1) - \delta r(x_1, \bar{y}) = 0 \tag{35d}$$

$$h(\bar{y}) = [\bar{\theta}(\bar{x}_{2e} - \bar{y}) - \eta(\bar{y} - \bar{x}_{2c}) + (\delta/2) r(x_1, \bar{y})]/\eta = 0 \tag{35e}$$

In vector form, the unique SS solution (35a-c) of the CL statics (27) are written as

$$\bar{\boldsymbol{x}} = \boldsymbol{\beta}(\bar{y}),\ \bar{\boldsymbol{x}} = (\bar{\boldsymbol{z}}^T, 0)^T,\ \bar{y} = \boldsymbol{c}_z \bar{\boldsymbol{z}} \quad \bar{\boldsymbol{z}} \in S_z \tag{36ab}$$

where

$$\boldsymbol{\beta}(\bar{y}) = [m(\bar{y}), \bar{y}, h(\bar{y})]^T,\ m:\ (35d),\ h:\ (35e) \tag{36c}$$

is the single-valued setpoint-to-SS ($\bar{y}$-to-$\bar{\boldsymbol{x}}$) NL bifurcation map.

From the application of the Hurwitz stability criterion (Boyce and Di Prima, 1967), the next proposition follows

**Proposition 2.** (Proof in Appendix A). The unique CL SS $\bar{\boldsymbol{x}}$ (36) is locally R stable if and only if the control gain $\boldsymbol{k}$ (12c) is chosen as

$$\boldsymbol{k} \in K_h = \{\boldsymbol{k} \in K | \boldsymbol{s}(\bar{y}, \boldsymbol{k}) >_r 0\},\ K:\ (12c) \tag{37a}$$

where ($s_1$, $s_2$ and $s_3$ are defined in Appendix A)

$$\boldsymbol{s}(\bar{y}, \boldsymbol{k}) >_r 0,\ \boldsymbol{s} = (s_1, s_2, s_3)^T,\ s_1, s_2, s_3:\ (A4) \tag{37b}$$

### 3.3. Closed-loop (CL) global monostability

According to Lyapunov stability theory (Abraham and Shaw, 1992; Hubbard and West, 1995), the CL deterministic system (26) with $\boldsymbol{k} \in \mathscr{K}_m$ (25b) is R $\bar{\boldsymbol{x}}$-monostable (without limit cycling) if and only if there is a (single-well shaped) *Lyapunov function* (with minimum $\mathscr{L}^-$ at $\bar{\boldsymbol{x}}$)

$$V = \mathscr{L}(\boldsymbol{x}) > \mathscr{L}^- \ \forall\, \boldsymbol{x} \in X \backslash \bar{\boldsymbol{x}},\ \mathscr{L}(\bar{\boldsymbol{x}}) = \mathscr{L}^-,\ \nabla \mathscr{L}(\bar{\boldsymbol{x}}) = 0 \tag{38a}$$

that decreases along the state motions

$$\dot{V} = [\nabla \mathscr{L}(\boldsymbol{x})] \boldsymbol{f}(\boldsymbol{x}, \boldsymbol{k}, \boldsymbol{d}) < 0 \ \forall\, \boldsymbol{x} \in X \backslash \bar{\boldsymbol{x}},\ \dot{V} = 0 \ @\ \boldsymbol{x} = \bar{\boldsymbol{x}},\ \boldsymbol{k} \in \mathscr{K}_m:\ (25b) \tag{38b}$$

with exponentially ultimately bounded (EUB) motions (Khalil, 2002; Sontag, 2008)

$$|\widetilde{\boldsymbol{x}}(t)| \le a_x e^{-\lambda_x t} |\widetilde{\boldsymbol{x}}_o|^+ + b_x |\widetilde{\boldsymbol{d}}|^+ \le |\widetilde{\boldsymbol{x}}|^+,\ \widetilde{\boldsymbol{d}} = \boldsymbol{d} - \bar{\boldsymbol{d}} \tag{39a}$$

where

$$\widetilde{\boldsymbol{x}} = \boldsymbol{x}(t) - \bar{\boldsymbol{x}},\ \boldsymbol{x}(t):\ (28),\ a_x > 0,\ b_x = (a_x/\lambda_x) l_d^f > 0 \tag{39b}$$

$$\lambda_x = 1/t_x >_r 0,\ t_x:\ (21b),\ |\widetilde{\boldsymbol{x}}|^+ = a_x |\widetilde{\boldsymbol{x}}_o|^+ + b_x |\widetilde{\boldsymbol{d}}|^+ \tag{39c}$$

$$|\boldsymbol{f}(\boldsymbol{x}, \boldsymbol{d}) - \boldsymbol{f}(\bar{\boldsymbol{x}}, \bar{\boldsymbol{d}})| \le l_x^f |\boldsymbol{x} - \bar{\boldsymbol{x}}| + l_d^f |\widetilde{\boldsymbol{d}}| \ \forall\, \boldsymbol{x} \in X \tag{39d}$$

$|\ |$ is the vector Euclidian norm, and $l_d^f$ is the Lipschitz constant of $\boldsymbol{f}$ with respect to $\boldsymbol{d}$. In this case, the CL deterministic system (26) is said to be R monostable.

**Proposition 3.** The CL deterministic dynamics (26) over $X$ are globally R monostable if and only if the control gain (12c) is chosen to that

$$\boldsymbol{k} \in K_m = \{\boldsymbol{k} \in K | \Im_{x =_r \bar{\boldsymbol{x}}}\} \subseteq K_h,\ K_h:\ (37) \tag{40a}$$

where

$$\bar{\boldsymbol{x}} = (\bar{\boldsymbol{z}}^T, 0)^T,\ \bar{\boldsymbol{z}} \in \mathscr{E}_z,\ \mathscr{E}_z:\ (11d)\ \boldsymbol{c}_z(\bar{\boldsymbol{z}}) = \bar{y} \tag{40b}$$

If admissible size ($|\widetilde{\boldsymbol{x}}_o|^+$ and $|\widetilde{\boldsymbol{d}}|^+$) deviations produce amissible state size ($|\widetilde{\boldsymbol{x}}|^+$) excursions about the nominal SS $\bar{\boldsymbol{x}}$, the CL deterministic system (26) is called practically (P) monostable (La Salle and Lefschetz, 1961).

According to Proposition 3, the control gain must be chosen with Hurwitz' suggestive criterion $\boldsymbol{k} \in K_h$ (37) followed by conclusive fine tuning $\boldsymbol{k} \in \mathscr{K}_m$ (25b) through numerical simulation of the CL deterministic ODE (26).

## 4. Closed-loop state PDF dynamics

In this section, the CL state PDF motion dynamics are characterized in terms of stationary R monomodality, deterministic-diffusion time scale, and MP state and its covariance evolutions. A gain condition for CL state PDF RM stability (25) is derived, the open-to-closed loop spatiotemporal geometric PDF change is discussed, and it is established that state PDF RM stability implies a R (EUB) version of state IP stability (17) (Wu et al, 2018a,b; Lu et al., 2022).

The dynamic FP PDE (19) is written; (i) in detailed form as

$$\begin{aligned} \partial_t \pi \ =\ & \partial_{x_1}\left[\frac{1}{2} q_1 \partial_{x_1} \pi - f_1(\boldsymbol{x}, \boldsymbol{d}) \pi\right] + \partial_{x_2}\left[\frac{1}{2} q_2(k_p) \partial_{x_2} \pi + \frac{1}{2} q_c(\boldsymbol{k}) \partial_{x_3} \pi - f_2(\boldsymbol{x}, \boldsymbol{d}, k_p) \pi\right] \\ & + \partial_{x_3}\left[\frac{1}{2} q_3(\boldsymbol{k}) \partial_{x_3} \pi + \frac{1}{2} q_c(\boldsymbol{k}) \partial_{x_2} \pi - f_3(\boldsymbol{x}, k_I) \pi\right],\ q_1, q_2\, q_3, q_c:\ (14j) \end{aligned} \tag{41a}$$

$$\pi(x_1, x_2, x_3, 0) = \pi_o(x_1, x_2, x_3),\ \int_{x_1^-}^{x_1^+} \int_{x_2^-}^{x_2^+} \int_{x_3^-}^{x_3^+} \pi(x_1, x_2, x_3, t) dx_1 dx_2 dx_3 = 1 \tag{41bc}$$

$$\begin{aligned} & \left[\frac{1}{2} q_1 \partial_{x_1} \pi - f_1(\boldsymbol{x}, \boldsymbol{d}) \pi\right]_{x_1^\pm} = 0, \\ & \left[\frac{1}{2} q_2(k_p) \partial_{x_2} \pi + \frac{1}{2} q_c(\boldsymbol{k}) \partial_{x_3} \pi - f_2(\boldsymbol{x}, \boldsymbol{d}, k_p) \pi\right]_{x_2^\pm} = 0 \end{aligned} \tag{41de}$$

$$\left[\frac{1}{2} q_3(\boldsymbol{k}) \partial_{x_3} \pi + \frac{1}{2} q_c(\boldsymbol{k}) \partial_{x_2} \pi - f_3(\boldsymbol{x}, k_I) \pi\right]_{x_3^\pm} = 0 \tag{41f}$$

and (ii) in *transport-reaction* form as (Alvarez et al., 2018)

$$\begin{aligned} \partial_t \pi \ =\ & \frac{1}{2} \nabla^T \boldsymbol{Q}(\boldsymbol{k}) \nabla \pi - \boldsymbol{f}(\boldsymbol{x}, \boldsymbol{d}, \boldsymbol{k}) \cdot \nabla \pi + [\nabla \cdot \boldsymbol{f}(\boldsymbol{x}, \boldsymbol{d}, \boldsymbol{k})] \pi, \\ & \boldsymbol{x} \in \mathscr{I}_{\mathscr{X}},\ \boldsymbol{Q}:\ (14h),\ \boldsymbol{f}:\ (15c) \end{aligned} \tag{42a}$$

$$\frac{1}{2} \boldsymbol{Q}(\boldsymbol{k}) \nabla \pi - \boldsymbol{f}(\boldsymbol{x}, \boldsymbol{d}, \boldsymbol{k}) \pi = 0,\ \boldsymbol{x} \in \mathscr{B}_{\mathscr{X}},\ \pi(\boldsymbol{x}, 0) = \pi_o(\boldsymbol{x}),\ \int_{\mathscr{X}} \pi(\boldsymbol{x}, t) d\boldsymbol{x} = 1 \tag{42b}$$

From a chemical reactor engineering perspective, the CL reactor CL FP PDE (42) describes the dynamic conservation of probability over the tridimensional space $\mathscr{X}$ with impermeable bounday $\mathscr{B}_{\mathscr{X}}$, and rate of change terms [in the RHS of (42a)] due to: (i) *Fick-like linear* transport $(1/2) \nabla^T \boldsymbol{Q} \nabla \pi$ with *allotropic diffusion* matrix $\boldsymbol{Q}$, (ii) *convective transport* $\boldsymbol{f} \cdot \nabla \pi$ with nonlinear space-dependent flow field $\boldsymbol{f}$, and (iii) *1st-order reaction-like probability generation* $(\nabla \cdot \boldsymbol{f}) \pi$ proportional to the probability "concentration" $\pi$ and with NL dependency on the "position" $\boldsymbol{x}$. The 3-dimensional FP PDE (42) can be solved numerically with specialized methods (LeVeque, 1992) or software packages (e.g., Ansys®, Comsol Multiphysics®).

According to FP PDE theory (Risken, 1996; Markowich and Villani, 2000; Frank, 2006): (i) the stationary FP PDE (23) associated to the simple CL dynamic FP PDE (41) has a unique stationary state (in general monomodal or non-monomodal) PDF solution $\bar{\pi}(\boldsymbol{x})$ (22), (ii) the state

PDF motions (18) R converge (25) to the stationary state PDF $\bar{\pi}(\boldsymbol{x})$, (iii) that R stationary state PDF monomodality [(24a) with $\mathscr{E}=_r\bar{\boldsymbol{x}}_m=\bar{\boldsymbol{x}}$] R precludes metastability over time scale $t_e$ (21b), and (iv) consequently, the next proposition follows.

**Proposition 4.** The CL PDF dynamics (42) is RM stable (25) if and only if the associated CL stationary state PDF (22) is R monomodal.

### 4.1. Robust stationary state PDF monomodality

Here, the correspondence between CL stochastic stationary state PDF monomodality and deterministic monostability is established by combining the characterizations of: (i) deterministic monostability with Lyapunov theory (38), and (ii) the stationary state PDF with the fluctuation dissipation relationship (Ao, 2003; Kwon et al., 2005; Wang et al., 2006) with functional analysis tools (Markowich and Villani, 2000; Frank, 2006).

In Boltzmann-Gibbs form, the unique state PDF solution of the stationary FP PDE (42) is given by (Wang et al., 2006)

$$\bar{\pi}(\boldsymbol{x})=ae^{-\phi(\boldsymbol{x})},\ \boldsymbol{x}\in\mathscr{X},\ \nabla\phi(\boldsymbol{x})=-\boldsymbol{G}^{-1}(\boldsymbol{x})\boldsymbol{f}(\boldsymbol{x},\bar{\boldsymbol{d}}),\ \det\boldsymbol{G}\neq 0 \tag{43ab}$$

where $a$ is a normalization constant, and the 9-entry of the 3x3 matrix $\boldsymbol{G}$ satisfies: (i) the fluctuation-dissipation relationship (with 9 algebraic equations)

$$\boldsymbol{G}(\boldsymbol{x})+\boldsymbol{G}^T(\boldsymbol{x})=\boldsymbol{Q}(\boldsymbol{k}) \tag{43c}$$

and (ii) the irrotationality condition (with 3 hyperbolic linear PDEs):

$$\nabla\times\left[\boldsymbol{G}^{-1}(\boldsymbol{x})\boldsymbol{f}(\boldsymbol{x},\bar{\boldsymbol{d}})\right]=0 \tag{43d}$$

When the stationary state PDF

$$\bar{\pi}(\boldsymbol{x})<\bar{\pi}^+=\bar{\pi}(\bar{\boldsymbol{x}}_m)\ \forall\ \boldsymbol{x}\in\mathscr{X}\backslash\bar{\boldsymbol{x}}_m,\nabla\bar{\pi}(\bar{\boldsymbol{x}}_m)=0$$

is R $\bar{\boldsymbol{x}}_m$-monomodal (with maximum $\bar{\pi}^+$ at $\bar{\boldsymbol{x}}_m$): (i) by (43), the stochastic potential

$$\phi(\boldsymbol{x})=-\ln\bar{\pi}(\boldsymbol{x})/a>\phi^-=\phi(\bar{\boldsymbol{x}}_m)\ \forall\ \boldsymbol{x}\in\mathscr{X}\backslash\bar{\boldsymbol{x}}_m,\ \nabla\phi(\bar{\boldsymbol{x}}_m)=0 \tag{44}$$

is single-well shaped (with minimum $\phi^-$ at $\bar{\boldsymbol{x}}_m$), and (ii) the deterministic system (26) can be expressed in gradient form (Hirsch and Smale, 1974)

$$\dot{\boldsymbol{x}}=-\boldsymbol{G}(\boldsymbol{x})\nabla\phi(\boldsymbol{x}),\ \boldsymbol{x}(0)=\boldsymbol{x}_o \tag{45a}$$

with the stochastic potential (44) as Lyapunov function

$$V=\mathscr{L}(\boldsymbol{x}):=\phi(\boldsymbol{x}),\ \phi:\ (44) \tag{45b}$$

$$\dot{V}=-\nabla^T\phi(\boldsymbol{x})[\boldsymbol{Q}(\boldsymbol{k})]\nabla\phi(\boldsymbol{x})\leq 0,\ \dot{V}=0\Leftrightarrow\bar{\boldsymbol{x}}=\bar{\boldsymbol{x}}_m \tag{45c}$$

From the stochastic Boltzmann-Gibbs PDF (43) and the deterministic Lyapunov (38) characterizations the next proposition follows.

**Proposition 5.** The CL stationary state PDF $\bar{\pi}(\boldsymbol{x})$ (43) is R monomodal if and only if the CL deterministic system (26) is globally R monostable. •

Differently from a previous study (Alvarez et al., 2018) on the OL 2-state stochastic reactor (3) where the correspondence between state PDF monomodality and deterministic monostability was established with the analytic solution of the 2D FP PDE (10), here the same correspondence for the 3-state CL stochastic reactor (15) has been obtained (Proposition 5) with a direct method that: (i) combines stochastic fluctuation-dissipation (43) and deterministic Lyapunov stability (38), and (ii) does not require the difficult or infeasible task of analytically solving the 3D FP PDE (42).

Proposition 5 states that, by the action of the PI control (12a) with adequate gain $\boldsymbol{k}\in\mathscr{K}_m$ (25b): the (in general) complex 2-state OL stationary PDF $\bar{\varsigma}(z)$ (11a) (with extremum of interest $\bar{z}$ that is a maximum, minimum or saddle) becomes a CL simple stationary R monomodal 3-state PDF $\bar{\pi}(\boldsymbol{x})$ (43) with mode at the prescribed value $\bar{\boldsymbol{x}}_m=\bar{\boldsymbol{x}}$ (24c).

### 4.2. State PDF stability

As direct consequence of Propositions 4 and 5 the next one follows

**Proposition 6.** The CL state PDF dynamics (42) is RM stable (25) if and only if the CL deterministic system (26) is R monostable, which happens the case if the control gain $\boldsymbol{k}$ is chosen as

$$\boldsymbol{k}\in\mathscr{K}_m=K_m\subseteq K_h,\ \mathscr{K}_m:\ (25b),\ K_m:\ (40a),\ K_h:\ (37a) \tag{46}$$

The CL stationary state PDF $\bar{\pi}(\boldsymbol{x})$ (43) with gain $\boldsymbol{k}\in\mathscr{K}_m$ (46) is R monomodal with most probable state $\bar{\boldsymbol{x}}_m$ equal to the unique SS $\bar{\boldsymbol{x}}$ of the CL deterministic R $\bar{\boldsymbol{x}}$-monostable dynamics (26), according to the expressions

$$\mathscr{E}=_r\bar{\boldsymbol{x}}_m=\bar{\boldsymbol{x}}=_r\mathfrak{S}_x,\ \boldsymbol{x}_m:\ (20b),\ \mathscr{E}:\ (24a),\ \mathfrak{S}_x:\ (29a),\ \bar{\boldsymbol{x}}:\ (36) \tag{47}$$

where $\mathscr{E}$ is the stationary extremum set of the stochastic CL stationary state PDF $\bar{\pi}(\boldsymbol{x})$ (43), and $\mathfrak{S}_x$ is the limit set of the associated deterministic CL dynamics (26).

When the CL state PDF motions (18) are RM stable (25), the mode ($\widetilde{\boldsymbol{x}}_m$) and control ($\widetilde{\boldsymbol{u}}_m$) deviations are EUB as

$$|\widetilde{\boldsymbol{x}}_m(t)|\leq l_{\boldsymbol{x}_m}^{\boldsymbol{m}_x}\left(a_\pi e^{-\lambda_\pi t}|\widetilde{\boldsymbol{\pi}}_o|_H^+ + b_\pi|\widetilde{\boldsymbol{d}}|^+\right)\leq l_{\boldsymbol{x}_m}^{\boldsymbol{m}_x}|\widetilde{\boldsymbol{\pi}}|_H^+ \tag{48a}$$

$$|\widetilde{\boldsymbol{u}}_m(t)|\leq l_{\boldsymbol{x}_m}^{\boldsymbol{c}_u}\left(a_\pi e^{-\lambda_\pi t}|\widetilde{\boldsymbol{\pi}}_o|_H^+ + b_\pi|\widetilde{\boldsymbol{d}}|^+\right)\leq l_{\boldsymbol{x}_m}^{\boldsymbol{c}_u}|\widetilde{\boldsymbol{\pi}}|_H^+ \tag{48b}$$

where

$$\widetilde{\boldsymbol{x}}_m=\boldsymbol{x}_m(t)-\bar{\boldsymbol{x}},\ \boldsymbol{m}_x(\bar{\boldsymbol{\pi}})=\bar{\boldsymbol{x}}_m=\bar{\boldsymbol{x}},\ |\boldsymbol{m}_x(\boldsymbol{\pi})-\boldsymbol{m}_x(\bar{\boldsymbol{\pi}})|\leq l_{\boldsymbol{\pi}}^{\boldsymbol{m}_x}|\widetilde{\boldsymbol{\pi}}| \tag{48c}$$

$$\widetilde{\boldsymbol{u}}_m=\boldsymbol{u}_m(t)-\bar{\boldsymbol{u}},\ \boldsymbol{m}_u(\bar{\nu}_m)=\bar{\boldsymbol{u}}_m=\bar{\boldsymbol{u}},|\boldsymbol{m}_u(\boldsymbol{x}_m)-\boldsymbol{m}_u(\bar{\boldsymbol{x}}_m)|\leq k_{\boldsymbol{x}_m}^{\boldsymbol{c}_u}|\widetilde{\boldsymbol{x}}_m|,\ k_{\boldsymbol{x}_m}^{\boldsymbol{c}_u}=\left(1+k_p^2\right)^{1/2} \tag{48d}$$

Proposition 6 (R stationary PDF monomodality) and inequality (48) (R state PDF stability) state that, by the action of the PI control (12a) with gain $\boldsymbol{k}\in\mathscr{K}_m$ (46): (i) the (in general) complex 2-state OL stationary state PDF $\bar{\varsigma}(z)$ (11) (with extremum of interest $\bar{z}$ that is a maximum, minimum or saddle) becomes a CL simple stationary R monomodal 3-state PDF $\bar{\pi}(\boldsymbol{x})$ (43) with prescribed mode $\bar{\boldsymbol{x}}_m=\bar{\boldsymbol{x}}$ (24c), and (ii) the OL transient (deterministic-diffusion-metastability) triscale (11c) becomes the CL OL transient (deterministic-diffusion) biscale (21b).

### 4.3. Random state motion in-probability (IP) stability

Here, it is shown that RM state PDF motion (18) stability (25) implies the R (EUB) version of random state motion IP stability (17) (Wu et al., 2018a,b; Lu et al., 2022).

Consider the family of nested subsets

$$\mathscr{X}_r=\{\boldsymbol{x}\in\mathscr{X}|\ |\boldsymbol{x}-\bar{\boldsymbol{x}}|\leq r,\ 0<r\leq r^+\},\ \mathscr{X}_r\cup\mathscr{X}_r^c=\mathscr{X} \tag{49ab}$$

of the probabilistic space $\mathscr{X}$ of the FP PDE (42), where

$$r=rad(\mathscr{X}_r,\bar{\boldsymbol{x}})=\max_{\boldsymbol{x}\in\mathscr{X}_r}|\boldsymbol{x}-\bar{\boldsymbol{x}}|,\ r^+=rad(\mathscr{X},\bar{\boldsymbol{x}}) \tag{50ab}$$

is the radius of $\mathscr{X}_r$ centered at $\bar{\boldsymbol{x}}$, and $\mathscr{X}_r^c$ is the complement of $\mathscr{X}_r$. Denote the probability $p$ (or $q$) of having (or not having) the state $\boldsymbol{x}(t)$ in $\mathscr{X}_r$ by

$$p(t,r)=\int_{\mathscr{X}_r}\pi(\boldsymbol{x},t),\ q(t,r)=\int_{\mathscr{X}_r^c}\pi(\boldsymbol{x},t)d\boldsymbol{x},\ p(t,r)+q(t,r)=1 \tag{51ac}$$

and express $q$ as

$$q(t,r) = \bar{q}(r) + \widetilde{q}(t,r),\ 0 \le \bar{q}(r) = \int_{\mathscr{X}_r^c} \bar{\pi}(\boldsymbol{x})d\boldsymbol{x} \le 1 \tag{52ab}$$

where

$$\widetilde{q}(t,r) = \int_{\mathscr{X}_r^c} \widetilde{\pi}(\boldsymbol{x},t)d\boldsymbol{x} \Rightarrow |\widetilde{q}(t,r)| \le l_{\bar{\pi}}^{\bar{q}}(r)|\widetilde{\pi}|_H^+,\ |\widetilde{\pi}|_H^+ :\ (25d) \tag{52cd}$$

is Lipschitz bounded.

The substitution of (51a), (52) and (25a) in (51c) yields the R (EUB with respect to nonvanishing noise and deterministic input disturbances) version of IP stability [(17) with $\epsilon_p$ replaced by $\epsilon(t,r)$]

$$p(t,r) \ge 1 - \epsilon(t,r),\ 0 \le \epsilon(t,r) \le 1 \tag{53ab}$$

where

$$\epsilon(t,r) = \bar{q}(r) + l_{\bar{\pi}}^{\bar{q}}(r)\left[a_\pi e^{-\lambda_\pi t}||\widetilde{\pi}_o(\boldsymbol{x})|_H^+ + b_\pi|\widetilde{\boldsymbol{d}}|^+\right],\ |\widetilde{\pi}_o(\boldsymbol{x})|_H^+ :\ (25c) \tag{53c}$$

This result is stated next in proposition form.

**Proposition 7.** CL state PDF RM stability (25) implies the EUB generalization (53) of IP stability (17).

According to Proposition 7 FP PDE-based PDF motion RM stability (25) is more general than SDE-based random state motion IP stability (17) (Wu et al., 2018a,b; Lu et al., 2022). This is so because the state PDF motions (18) of the FP PDE (42) contain the complete probabilistic information on the random motion bundle set (16) of the associated SDE (15).

Thus, Proposition 7: (i) introduces an improved R [EUB over time biscale $(t_x, t_d)$ (21b)] version (53) of IP stability (17) [over time monoscale $t_x$ (21b)], and (ii) opens an avenue for fruitful complementation between the SDE (15) (MC method-like) and FP PDE (42) simulation approaches.

More on the subject of state R IP stability in the light of PDF RM stability with be discussed in Section 6 on "Illustration with indicative examples".

## 5. State and control mode evolutions

Here the state and control modes and their covariance evolutions are: (i) characterized according to the FP PDE (42), and (ii) approximated in a P sense with an ODE.

### 5.1. FP PDE-based mode evolution

The state PDF mode evolution $\boldsymbol{x}_m$ and its rate of change $\boldsymbol{v}_m$ are determined by the FP PDE (42) (Jazwinski, 1970) with the output map (54b):

$$\partial_t \pi = \mathscr{F}(\pi, \boldsymbol{d}),\ \boldsymbol{B}(\pi, \boldsymbol{d}) = 0,\ \pi(0) = \pi_o(\boldsymbol{x}) \tag{54a}$$

$$\boldsymbol{x}_m = \boldsymbol{m}_x(\pi),\ u_m = \boldsymbol{c}_u(\boldsymbol{x}_m) \tag{54b}$$

In a way that is analogous to the way in which a geometric NLSF controller is constructed (Isidori, 1999) and along FP PDE analysis ideas (Jazwinski, 1970), the time derivation of the output map $\boldsymbol{m}_x$ along the state PDF motion $\pi$ yields the next proposition in terms the NL vector

$$\varrho_\pi(\boldsymbol{x}_m, \boldsymbol{d}) = [\varrho(\pi, \boldsymbol{d})]_{\boldsymbol{x}=\boldsymbol{x}_m},\ \varrho_{\bar{\pi}}(\bar{\boldsymbol{x}}_m, \bar{\boldsymbol{d}}) = 0,\ \bar{\boldsymbol{x}}_m = \bar{\boldsymbol{x}} \tag{55a}$$

$$|\varrho_\pi(\pi, \boldsymbol{d})| \le l_{\boldsymbol{x}_m}^{\varrho_\pi}|\widetilde{\boldsymbol{x}}_m| + l_{\boldsymbol{d}}^{\varrho_\pi}|\widetilde{\boldsymbol{d}}|,\ l_{\boldsymbol{x}_m}^{\varrho_\pi} = l_\pi^\varrho\, l_{\boldsymbol{x}_m}^\pi|\widetilde{\boldsymbol{x}}_m|^+,\ l_{\boldsymbol{x}_m}^\pi = \lambda_H^+ + k_{\boldsymbol{x}_m}^o,\ l_{\boldsymbol{d}}^{\varrho_\pi} = l_\pi^\varrho\, l_{\boldsymbol{d}}^\pi \tag{55b}$$

where

$$\varrho(\pi, \boldsymbol{d}) = (\boldsymbol{H}\pi)^{-1}\{[\boldsymbol{H}\boldsymbol{f}(\boldsymbol{x}, \boldsymbol{d})]\pi - (1/2)\boldsymbol{H}(\boldsymbol{Q}\nabla\pi)\},\ \varrho(\bar{\pi}, \bar{\boldsymbol{d}}) = 0,\ \nabla, \boldsymbol{H} :\ (20e) \tag{55c}$$

$$|\varrho(\pi, \boldsymbol{d})| \le l_\pi^\varrho|\widetilde{\pi}|_H^+ + l_{\boldsymbol{d}}^\varrho|\widetilde{\boldsymbol{d}}|,\ \varrho(\pi, \boldsymbol{d}) = 0\ \textit{if}\ \pi\ \textit{is symmetric},\ \boldsymbol{Q} :\ (14h) \tag{55d}$$

$\varrho_\pi$ vanishes at $(\bar{\boldsymbol{x}}_m, \bar{\boldsymbol{d}})$, and $\varrho$ depends in a complex way (through up to 2nd and 3rd-order partial derivatives of the convective field $\boldsymbol{f}$ and the state PDF $\pi$, respectively) on the PDF geometry at $\boldsymbol{x}_m$.

**Proposition 8.** (Proof in Appendix B). The R convergent state (56a) and control (56b) mode evolutions satisfy the ODE-based system [driven through $\varrho_\pi$ by driven by the state PDF $\pi$ of the FP PDE (42)]

$$\dot{\boldsymbol{x}}_m = \boldsymbol{f}(\boldsymbol{x}_m, \boldsymbol{d}) + \varrho_\pi(\boldsymbol{x}_m, \boldsymbol{d}),\ \boldsymbol{x}_m(0) = \boldsymbol{x}_{mo};\ u_m = \boldsymbol{c}_u(\boldsymbol{x}_m) \tag{56ab}$$

where

$$\boldsymbol{x}_{mo} = \boldsymbol{m}_x(\pi_o),\ \boldsymbol{f} :\ (14e-f)\ \varrho_\pi :\ (55a),\ \boldsymbol{m}_x :\ (20b),\ \boldsymbol{c}_u :\ (14g)$$

According to (56a), the state mode rate of change $(\boldsymbol{f} + \varrho_\pi)$ depends on the state PDF $\pi$ of the FP PDE (54a), and has two components: (i) the deterministic vector field $\boldsymbol{f}$ (14) that does not depend on $\pi$, and (ii) the term $\varrho_\pi$ (55) that depends on the geometry of $\pi$ at the state mode $\boldsymbol{x}_m$. According to (56b), the control mode $u_m$ is an output of the ODE (56a) driven by $\pi$.

From the application (Gonzalez and Alvarez, 2005; Franco-de los Reyes and Alvarez, 2022) of Lyapunov's Converse Theorem (Vidyasagar, 1993) to (56a) the next proposition follows, with the definitions

$$l_m = \lambda_x - a_x l_{\boldsymbol{x}_m}^{\varrho_\pi} > 0,\ \lambda_\pi < l_m < \lambda_x,\ \widetilde{\boldsymbol{x}}_m = \boldsymbol{x}_m - \bar{\boldsymbol{x}}_m,\ l_{\boldsymbol{x}_m}^{\varrho_\pi} :\ (55b) \tag{57a}$$

$$b_m = \left(l_{\boldsymbol{d}}^f + l_{\boldsymbol{d}}^{\varrho_\pi}\right)/l_m,\ |\widetilde{\boldsymbol{x}}_m|^+ = a_x|\widetilde{\boldsymbol{x}}_{mo}|^+ + b_m|\widetilde{\boldsymbol{d}}|^+,\ l_{\boldsymbol{d}}^f :\ (39d) \tag{57b}$$

where

$$\varrho_\pi = 0 \Rightarrow (l_m, b_m) = (\lambda_x, b_x),\ (\lambda_x, b_x) :\ (41b-c) \tag{57c}$$

**Proposition 9.** (Proof in Appendix C). The R convergent state (58a) and control (58b) mode evolutions are R (EUB) stable, according to the inequalities:

$$|\widetilde{\boldsymbol{x}}_m(t)| \le a_x e^{-l_m t}|\widetilde{\boldsymbol{x}}_{mo}|^+ + b_m|\widetilde{\boldsymbol{d}}|^+ \le |\widetilde{\boldsymbol{x}}_m|^+,\ l_m : (57a) \tag{58a}$$

$$|\widetilde{u}_m(t)| \le l_{\boldsymbol{x}_m}^{\boldsymbol{c}_u}\left(a_x e^{-l_m t}|\widetilde{\boldsymbol{x}}_{mo}|^+ + b_m|\widetilde{\boldsymbol{d}}|^+\right) \le k_{\boldsymbol{x}_m}^{\boldsymbol{c}_u}|\widetilde{\boldsymbol{x}}_m|^+,\ k_{\boldsymbol{x}_m}^{\boldsymbol{c}_u} :\ (48d) \tag{58b}$$

where

$$\widetilde{\boldsymbol{x}}_m = \boldsymbol{x}_m - \bar{\boldsymbol{x}},\ \bar{\boldsymbol{x}}_m = \bar{\boldsymbol{x}},\ \widetilde{u}_m = u_m - \bar{u},\ b_m :\ (57c) \tag{58c}$$

The R stability bounding (58): (i) is less conservative than its state PDF-based counterpart (55), and (ii) states that, in the limit when $\varrho_\pi$ vanishes, the state and control modes evolve along deterministic time scale $l_m = t_x = \lambda_x$ with gain $b_m = b_x$ $[(\lambda_x, b_x) : (39b\text{-}c)]$.

### 5.2. Approximated mode and variability evolutions

Motivated by the preceding developments, let us enforce $\varrho_\pi = 0$ in the ODE (56a) to obtain its approximation:

$$\dot{\widehat{\boldsymbol{x}}}_m = \boldsymbol{f}(\widehat{\boldsymbol{x}}_m, \boldsymbol{d}),\ \widehat{\boldsymbol{x}}_m(0) = \widehat{\boldsymbol{x}}_{mo} \approx \boldsymbol{x}_{mo},\ \boldsymbol{f}(\bar{\widehat{\boldsymbol{x}}}_m, \bar{\boldsymbol{d}}) = 0 \tag{59a}$$

with solution motions

$$\widehat{\boldsymbol{x}}_m = \boldsymbol{\tau}_x[t, \widehat{\boldsymbol{x}}_{mo}, \boldsymbol{d}(t)],\ \widehat{u}_m = \boldsymbol{c}_u(\widehat{\boldsymbol{x}}_m) \tag{59b}$$

which, by-construction, (59) are R stable over time scale $t_x$, with EUB inequality

$$|\boldsymbol{e}_m(t)| \le a_x e^{-\lambda_x t}|\boldsymbol{e}_{mo}|^+ + b_x|\widetilde{\boldsymbol{d}}|^+ \le |\boldsymbol{e}_m|^+,\ \lambda_x \approx 1/t_x,\ t_x :\ (21b),\ b_x :\ (39b) \tag{60a}$$

where

$$\boldsymbol{e}_m = \widehat{\boldsymbol{x}}_m(t) - \bar{\boldsymbol{x}}_m,\ \bar{\boldsymbol{x}}_m = \bar{\boldsymbol{x}},\ |\boldsymbol{e}_m|^+ = a_x|\boldsymbol{e}_{mo}|^+ + b_x|\widetilde{\boldsymbol{d}}|^+ \tag{60b}$$

Along the notion of practical stability "when admissible disturbance size cause admissible state deviation size" (LaSalle and Lefschetz, 1961), the R stable mode motion $\widehat{\boldsymbol{x}}_m$ (59) (over deterministic time scale) is said to be $\varepsilon$-practically ($\varepsilon$-P) convergent if the relative approximation error

$$e_r := \frac{||\widetilde{\boldsymbol{x}}_m|^+ - |\boldsymbol{e}_m|^+|}{|\widetilde{\boldsymbol{x}}_m|^+} \le \epsilon := 1\Big/N,\ |\widetilde{\boldsymbol{x}}_m|^+ :\ (57b),\ |\boldsymbol{e}_m|^+ :\ (60b) \tag{61}$$

is less than one in $N$.

This $\varepsilon$-P convergence property: (i) agrees with and explains the state mode evolutions over deterministic-like time scale obtained with FP PDE-based simulation in CL 1D isothermal (Baratti et al., 2018) and 2D biological (Schaum et al., 2021) reactors with proportional control.

The augmentation of (59a) with the cascaded Riccati matrix equation (62b) (Jazwinski, 1970) yields the approximated dynamics of the state ($\widehat{\boldsymbol{x}}_m$) and control ($\widehat{\sigma}_u$) modes as well of their covariances ($\widehat{\Sigma}_m$ and $\widehat{\sigma}_u$):

$$\dot{\widehat{\boldsymbol{x}}}_m = \boldsymbol{f}(\widehat{\boldsymbol{x}}_m, \boldsymbol{d}),\ \widehat{\boldsymbol{x}}_m(0) = \widehat{\boldsymbol{x}}_{mo} \approx \boldsymbol{x}_{mo} \tag{62a}$$

$$\begin{aligned}\dot{\widehat{\Sigma}}_m &= \boldsymbol{J}(\widehat{\boldsymbol{x}}_m, \boldsymbol{d})\widehat{\Sigma}_m + \widehat{\Sigma}_m\boldsymbol{J}(\widehat{\boldsymbol{x}}_m, \boldsymbol{d}) + \boldsymbol{Q},\ \widehat{\Sigma}_m(0) = \boldsymbol{\Sigma}_{mo}, \boldsymbol{J}(\widehat{\boldsymbol{x}}_m)\\ &= [\partial_{\boldsymbol{x}_m}\boldsymbol{f}(\widehat{\boldsymbol{x}}_m, \bar{\boldsymbol{d}}, \boldsymbol{k})]\end{aligned} \tag{62b}$$

$$\widehat{u}_m = \boldsymbol{c}_u\widehat{\boldsymbol{x}}_m,\ \widehat{\sigma}_u = \boldsymbol{v}_u(\mathrm{diag}\widehat{\Sigma}_m)\boldsymbol{v}_u^T \tag{62c}$$

with $\varepsilon$-P convergent motion and output

$$(\widehat{\boldsymbol{x}}_m, \widehat{\Sigma}_m)(t) \overset{\lambda_x}{\to} (\boldsymbol{x}_m, \boldsymbol{\Sigma}_m)(t),\quad (\widehat{u}_m, \widehat{\sigma}_u)(t) \overset{\lambda_x}{\to} (u_m, \sigma_u)(t),\quad \boldsymbol{x}_m, u_m, \sigma_u :\ (20) \tag{63}$$

and stationary regime

$$\bar{\widehat{\boldsymbol{x}}}_m = \bar{\boldsymbol{x}}_m = \bar{\boldsymbol{x}},\ \bar{\widehat{\Sigma}}_m = \bar{\Sigma}_m = \bar{\Sigma},\ \bar{\widehat{\sigma}}_u = \bar{\sigma}_u \tag{64ac}$$

$$\boldsymbol{f}(\bar{\boldsymbol{x}}_m, \bar{\boldsymbol{d}}) = 0,\ \bar{\boldsymbol{J}}\,\bar{\Sigma}_m + \bar{\Sigma}_m\bar{\boldsymbol{J}}^T + \boldsymbol{Q} = 0,\ \bar{\sigma}_u = \boldsymbol{v}_u(\mathrm{diag}\bar{\Sigma}_m)\boldsymbol{v}_u^T,\ \bar{\boldsymbol{J}} = \boldsymbol{J}(\bar{\boldsymbol{x}}_m) \tag{64dg}$$

where $\bar{\boldsymbol{x}}$ (or $\bar{\boldsymbol{x}}_m$) is the prescribed CL deterministic SS (or state PDF mode) (35a-c) or [(45c)].

The validity of the $\varepsilon$-P approximation (62) will be assessed (in Section 6 on case examples) with FP PDE simulation. The analytic dependencies of the stationary state ($\bar{\Sigma}$) and control ($\bar{\sigma}_u$) covariances on the control gains: (i) are listed in Appendix D, and (ii) will be employed in the next section to assist the gain tuning of the examples.

The $\varepsilon$-P MP state and control convergence expression (62) states that, by the action of the PI control (12a) with gain $\boldsymbol{k} \in \mathscr{K}_m$(25b): (i) the MP temperature ($x_{2m}$) and concentration ($x_{1m}$) states are regulated over almost deterministic time scale ($t_x$) with elimination (or attenuation) of MP temperature (or concentration) asymptotic offset due to change in the mean value of the exogenous stochastic disturbances $\boldsymbol{d}_s$ (8f). When the I action is eliminated from the PI control (12a), the resulting CL 2-state PDF $\varsigma(z,t)$-dynamics [(9) with $u = \bar{u} - k_p(y - \bar{y})$] remains R PDF stable with R $\bar{z}$-monomodal stationary state PDF $\bar{\varsigma}(z)$ (11a) and stationary mode at prescribed value $\bar{z}_m = \bar{z}$. In other words, with respect to P control, the PI control: (i) increases by one the dimension of the probabilistic state space, (ii) preserves the simplicity (state PDF RM stability) of the CL state PDF dynamics (42), and (iii) eliminates (or attenuates) MP state temperature (or concentration) offset due to persistent constant deterministic-stochastic disturbances.

### 5.3. Interpretation of the PI control within FP's stochastic modeling framework

As an important conceptual conclusion of the present study, here the industrial-type PI control for the exothermic reactor class (3) is interpreted within the FP theory-based modeling framework.

The CL stochastic dynamics of the industrial PI temperature controller (12) is an output (65c) of the CL FP PDE (65a):

$$\partial_t\pi = \mathscr{F}(\pi, \boldsymbol{d}),\ \boldsymbol{B}(\pi, \boldsymbol{d}) = 0,\ \pi(0) = \pi_o(\boldsymbol{x}),\ \nu(u,t) = h[\pi(\boldsymbol{x},t)] \tag{65ab}$$

$$u_m = PI(y_m),\ y_m = \boldsymbol{c}_y\boldsymbol{x}_m,\ \boldsymbol{x}_m = \boldsymbol{m}_x(\pi) \tag{65ce}$$

On the basis of the most probable temperature measurement $y_m$, the PI control (65d) applies the most probable value $u_m$ of the control PDF $\nu(u, t)$. The effect of mass-heat balance, actuator, and measurement noises is accounted for by the noise covariance matrix $\boldsymbol{Q}$ (14h) of the FP PDE (65a) that generates the state ($\pi$) and control ($\nu$) PDFs.

Hitherto, the technical developments have been executed with the standard notation employed in the literature: denoting the deterministic and random variables of the ODE (26) and SDE (15) with the same symbol set $\{u,\ \boldsymbol{x},\ \boldsymbol{y}\}$. In Table 2 the deterministic (12a) and stochastic (13) PI control variants are presented with explicitly differentiation of deterministic ($\boldsymbol{x}_d$) and random ($\boldsymbol{x}_s$) states.

## 6. Illustration with indicative examples

Here, the main theoretical developments and findings of Sections 3 to 5 are illustrated with: (i) analytic formula application, (ii) FP PDE (42) numerical simulation with finite volume method (Balzano et al., 2010), (iii) SDE (15) numerical simulation with MC-type method (Wu et al., 2018a,b). The CL behavior simulations in the presence of combined endogenous zero-mean and exogenous time-varying mean noise disturbances is performed along protocols employed in application oriented research (Wu et al., 2018a,b) and industrial practice (Franco-de los Reyes and Alvarez, 2022).

On the basis of previous studies (Alvarez et al., 2018; Franco-de los Reyes and Alvarez, 2022; Santamaria-Padilla et al., 2022), the OL 2-state stochastic reactor class (3) was set with: (i) reaction rate with first-order kinetics and Arrhenius temperature dependency, i.e.,

$$r(x_1, x_2) = x_1 e^{\varepsilon_a(1 - 1/x_2)},\ \varepsilon_a = E_a/\left(R_g T_r\right) = 25,\ \bar{x}_{1e} = \bar{x}_{2e} = \bar{x}_{2c} = 1 \tag{66ac}$$

and (ii) realistic (parasitic) background and instrument measurement noise standard deviations

$$\begin{aligned}\vartheta_1 &:= \sqrt{\gamma_1} = 1.14{\cdot}10^{-2},\ \vartheta_2 := \sqrt{\gamma_2} = 6.32{\cdot}10^{-3}\\ \vartheta_u &:= \sqrt{\gamma_u} = 0,\ \vartheta_y := \sqrt{q_y} = 2{\cdot}10^{-4}\end{aligned} \tag{67ad}$$

that determine the CL noise covariance $3 \times 3$ matrix $\boldsymbol{Q}(\boldsymbol{k})$ (14h).

Figure 1 shows that, over its Damköhler-Stanton ($\delta$-$\eta$) parameter space, the OL 2-state stochastic reactor (8) has regions of simple (monomodal) and complex (bimodal and vulcanoid) stationary 2-state PDF $\bar{\varsigma}(z)$ (11a). The monomodal, bimodal and vulcanoid stochastic state PDF regions correspond to regions of deterministic monostability, bistability, and limit cycling, respectively, delimited by saddle-node (S) (dashed line) and Hopf (H) (continuous line) bifurcation curves

**Table 2**
Deterministic and stochastic PI controls.

| PI control | Deterministic $u_d = PI(y_d)$ | Stochastic $u_s = PI(y_s + w_y) + \xi_u$ | $u_m = PI(y_m)$ |
|---|---|---|---|
| | $u_d,\ y_d$: deterministic | $u_s,\ y_s$: random | $u_m,\ y_m$: PDF modes |
| **Measurement** | $y_d = \boldsymbol{c}_y\boldsymbol{x}_d$ | $y_s = \boldsymbol{c}_y\boldsymbol{x}_s + \boldsymbol{w}_y$ | $y_m = \boldsymbol{c}_y\boldsymbol{x}_m$ |
| **Dynamics** | **ODE** (26): $\dot{\boldsymbol{x}}_d = \boldsymbol{f}(\boldsymbol{x}_d, \boldsymbol{d})$ $\boldsymbol{x}_d(0) = \boldsymbol{x}_{do}$ | **SDE** (15): $\dot{\boldsymbol{x}}_d = \boldsymbol{f}(\boldsymbol{x}_d, \boldsymbol{d}) + \boldsymbol{w}$ $\boldsymbol{x}_s(0) = \mathscr{R}[\pi_o(\boldsymbol{x}_s)]$ | **FP PDE** (42): $\boldsymbol{x}_m = \boldsymbol{m}_x(\pi)$ $\partial_t\pi = \mathscr{F}(\pi, \boldsymbol{d})$ $\boldsymbol{B}(\pi, \boldsymbol{d}) = 0$ $\pi(\boldsymbol{x}, 0) = \pi_o(\boldsymbol{x})$ |
| **State** | $\boldsymbol{x}_d$: deterministic | $\boldsymbol{x}_s$: random | $\pi$: PDF |

(Alvarez et al., 2018).

The tree indicative case examples listed in Table 3 (dots in Fig. 1) with complex (non-monomodal) OL PDFs and possibility of metastability (in cases $C_1$ and $C_2$) were chosen [geometric and denomination details can be seen in (Alvarez et al., 2018)].

- Case $C_1$ with OL fragile aloprobable bimodality (underlain by deterministic aloattractive bistability), and the least probable mode as target CL extremum.
- Case $C_2$ with OL robustly equiprobable bimodality (underlain by deterministic equiattractive bistability), and the almost null probable saddle as target CL extremum.
- Case $C_3$ with OL robust vulcanoid (underlain by a deterministic limit cycle), and the almost null probable bottom minimum as target CL extremum.

In the three cases, CL state PDF dynamics must be attained, with: (i) robustly monomodal stationary 3-state PDF $\bar{\pi}(\boldsymbol{x})$ with prescribed mode $\bar{\boldsymbol{x}}_m = \bar{\boldsymbol{x}}$ (45c) determined by the OL 2-state extremum $\bar{z}$ (4b), (ii) preclusion of metastability (21b), and (iii) an adequate compromise between state mode and variability regulation speed, robustness with respect to deterministic and stochastic disturbances, and control mode-variability effort.

The dependency of the stationary concentration ($\bar{s}_1$), temperature ($\bar{s}_2$), integral action ($\bar{s}_3$) state and control ($\bar{s}_u$) standard deviations (STDs)

$$(\bar{s}_1, \bar{s}_2, \bar{s}_3, \bar{s}_u)(\boldsymbol{k}) = (\sqrt{\bar{\sigma}_{11}}, \sqrt{\bar{\sigma}_{22}}, \sqrt{\bar{\sigma}_{33}}, \sqrt{\bar{\sigma}_u})(\boldsymbol{k}) \tag{68}$$

on PI gain vector $\boldsymbol{k}$ (12a) is given by the analytical solution (D3 in Appendix D) of the stationary Riccati equation (64e).

For application-oriented insight purpose, the proportional gain-reset time parametrization

$$\boldsymbol{\kappa} = \left(k_p, \tau_I\right)^T \in \mathscr{K}_h \subseteq \mathscr{K}_m \subset \mathscr{K}, \ \tau_I = k_p \Big/ k_I : \ (12c) \tag{69a}$$

of the proportional-integral gain vector $\boldsymbol{k}$ (12) will be employed, where

$$\begin{aligned} \mathscr{K}_h \ &= \ \boldsymbol{f}_{\boldsymbol{\kappa}}(K_h), \ \boldsymbol{\kappa} = \left(k_p, k_p/k_I\right)^T := \boldsymbol{f}_{\boldsymbol{\kappa}}(\boldsymbol{k}) \\ & \quad K : \ (12c), \ K_h : \ (37), \ \mathscr{K}_m : \ (25b) \end{aligned} \tag{69b}$$

For comparative visualization purposes, the graphical displays will be done for: (i) the single-state marginal concentration, temperature, integral action, and control (20f-g) PDFs of the CL $\boldsymbol{\kappa}$-dependent 3-state PDF (42), and (ii) the concentration-temperature marginal PDF

$$\bar{\varsigma}_c(z) := \int_{x_3^-}^{x_3^+} \bar{\pi}(\boldsymbol{x}) dx_3, \ \bar{\pi} : \ (43), \ \ \bar{\varsigma}(z) : \ (11a), \ x_3^- = -0.2, \ x_3^+ = 0.2 \tag{70}$$

and the OL 2-state PDF (11a).

Case $C_1$ will examined in detail, including: (i) stationary state PDF shape, stationary state and control PDF standard deviations (STDs) dependency on gain as well as mode and its covariance evolution, and dependency of the PDF evolution on gain. Due to space limitation, for Cases $C_2$ and $C_3$ only the stationary PDF shape and the dependency of the state and control STDs on gain will be presented.

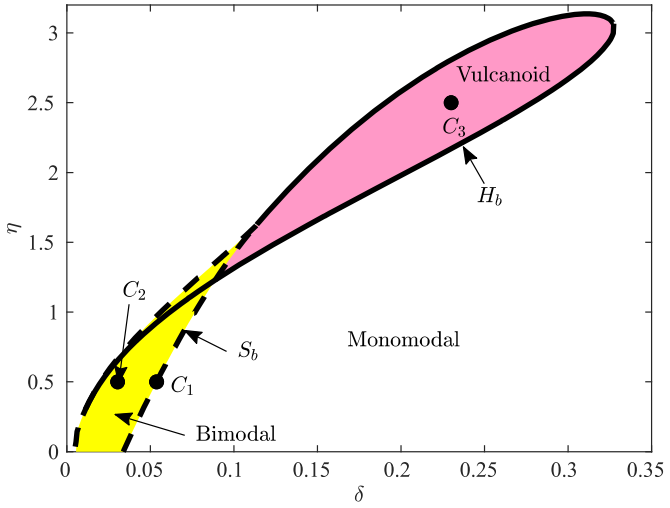


**Fig. 1.** Stationary state PDF [$\bar{\varsigma}(z)$ (11a)] behavior regions of the reactor class (3), in the Damköhler-Stanton parameter space delimited by deterministic saddle-node ($S_b$) (- - - -) and Hopf ($H_b$) (—) bifurcation: (i) monomodal (white), (ii) bimodal (yellow), and (iii) vulcanoid (pink). Indicative examples (Table 3) (•): (i) $C_1$ (fragile bimodality), (ii) $C_2$ (robust bimodality), and (iii) $C_3$ (robust vulcanoid).

### 6.1. Case $C_1$ (OL fragile bimodal PDF)

In Case $C_1$ (Fig. 1, Table 3): (i) the OL 2-state PDF is fragilely aloprobable bimodal with least probable mode $\bar{z}_{\bar{m}}$ as target extremum, and (ii) the controller must attain robust 3-state CL monomodality with most probable stationary state $\bar{\boldsymbol{x}}_m$ at the extremum $\boldsymbol{x}_{\bar{m}}$ associated with $\bar{z}_{\bar{m}}$.

#### 6.1.1. Gain selection

In Fig. 2 are presented the analytic dependencies on the gain $\boldsymbol{\kappa} \in \mathscr{K}_h$ (69) (green subset of the bottom gain plane $\mathscr{K}$), where the necessary Hurwitz conditions (37) are met, of the concentration ($\bar{s}_1$), temperature ($\bar{s}_2$), and control ($\bar{s}_u$) standard deviations (68) of the stationary CL covariance matrix $\bar{\Sigma}$ (64b), for three measurement noise STDs $\vartheta_y$: (i) = 0 (left column), (ii) = $2.00{\cdot}10^{-4}$ (67d) (center column, nominal value), and (iii) = $6.32{\cdot}10^{-4}$ (right column).

According to Fig. 2, for fixed integral reset time $\tau_I$, with the increase of the proportional gain $k_P$: (i) the concentration standard deviation $\bar{s}_1$ (first row) decreases, reaching an asymptotic value determined by the background concentration [$\vartheta_1$ (67a)] and temperature measurement [($\vartheta_y$) (67d)] noise STDs, (ii) the temperature standard deviation $\bar{s}_2$ (2nd row) initially decreases, reaches a minimum value, and then increases, (iii) and the control STD $\bar{s}_u$ (3rd row) grows with the gain. The increase of the temperature measurement STD $\vartheta_y$ makes more rapid and pronounced the changes. These FP theory-based results, agree with and explain: (i) common knowledge in industrial control practice (Samad, 2017), (ii) the results obtained before with MC SDE (15)-based simulation (Ratto, 1998; Ratto and Paladino, 2000).

Tight ($\boldsymbol{\kappa}_1^t$) and loose ($\boldsymbol{\kappa}_1^l$) gain pairs were considered

$$\boldsymbol{\kappa}_1^t = (4,1)^T \in \mathscr{K}_h, \ \boldsymbol{\kappa}_1^l = (1,1)^T \in \mathscr{K}_h, \ \mathscr{K}_h \subseteq \mathscr{K}_m : \ (69) \tag{71ab}$$

with: (i) $\boldsymbol{\kappa}_1^t$ chosen to get an adequate compromise between regulation speed, state and control effort variances (see bottom plane of Fig. 2, central column), and (ii) $\boldsymbol{\kappa}_2$ (with proportional gain four times slower, closer to the bifurcation boundary of the gain $\mathscr{K}_h$) chosen for comparison and analysis.

The gain $\boldsymbol{\kappa}_1^t$ (or $\boldsymbol{\kappa}_1^l$) is away from (or close to) the boundary $s(\bar{y}, \boldsymbol{\kappa}_i) = 0$ (37b) of the Hurwitz gain set $\mathscr{K}_h$ (69b) where mono-bimodal (Fig. 1) CL extremum bifurcation occurs by control gain change.

#### 6.1.2. OL and CL stationary state PDFs

With the tight gain $\boldsymbol{\kappa}_1^t$ (71a) and STD values (67), the OL (fragilely bimodal) stationary PDF (top panel) becomes the CL (robustly monomodal) concentration and temperature marginal PDF (bottom panel) $\bar{\varsigma}_c(z)$ (70) reported in Fig. 3, showing that, in agreement with the theoretical results (of Sections 3 to 5): in the open (top panel)-to-closed (bottom panel) loop passage, the least probable and nonunique 2-state OL mode $\bar{z}_m$ becomes the unique CL mode $\bar{\boldsymbol{x}}_m$ of the monomodal almost Gaussian stationary 3-state PDF. As expected, the loose gain $\boldsymbol{\kappa}_1^l$ (71b) (with PDFs not shown for lack of space) yields larger state

**Table 3**
OL 2-state and CL 3-state stationary PDF characteristics of the case examples.

| Case | | Stationary state PDF Open-loop | | | Closed-loop |
|---|---|---|---|---|---|
| | $\delta$: **Damköhler**<br>$\eta$: **Stanton** | | **Extremum set**: $\mathscr{E}_o$<br>**Setpoint:** $\bar{y} = \boldsymbol{c}_z\bar{\boldsymbol{z}}_m$ | **Target Extremum** | **Robust monomodal state PDF** |
| $C_1$ | $\delta = 0.0537$<br>$\eta = 0.5$ | **Bimodal**<br>Fragile Alo-probable | $\mathscr{E}_o = \{\bar{z}_m^-, \bar{z}_s, \bar{z}_m^+\}$<br>$\bar{z}_m^-$, $\bar{z}_m^+$: Highly probable modes<br>$\bar{y} = 1.05235$ (of $\bar{z}_m$) | $\bar{z}_m^-$:<br>Least probable mode | $\mathscr{E} = \bar{\boldsymbol{x}}_m$<br>$\bar{\boldsymbol{x}}_m = \begin{bmatrix} \bar{\boldsymbol{z}}_m \, 0 \end{bmatrix}$<br>$\bar{y} = \boldsymbol{c}_x\bar{\boldsymbol{x}}_m$ |
| $C_2$ | $\delta = 0.030903$<br>$\eta = 0.5$ | **Bimodal**<br>Robust Equiprobable | $\mathscr{E}_o = \{\bar{z}_m^-, \bar{z}_s, \bar{z}_m^+\}$<br>$\bar{z}_m^-$, $\bar{z}_m^+$: Highly probable modes<br>$\bar{y} = 1.15227$ (of $\bar{z}_s$) | $\bar{z}_s$:<br>Almost null probable saddle | |
| $C_3$ | $\delta = 0.23$<br>$\eta = 2.5$ | **Vulcanoid**<br>Robust | $\mathscr{E}_o = \{\bar{z}_m, \boldsymbol{l}\}$<br>$\boldsymbol{l}$: Highly probable rim<br>$\bar{y} = 1.09627$ (of $\bar{z}_m$) | $\bar{z}_m$:<br>Almost null probable bottom | |

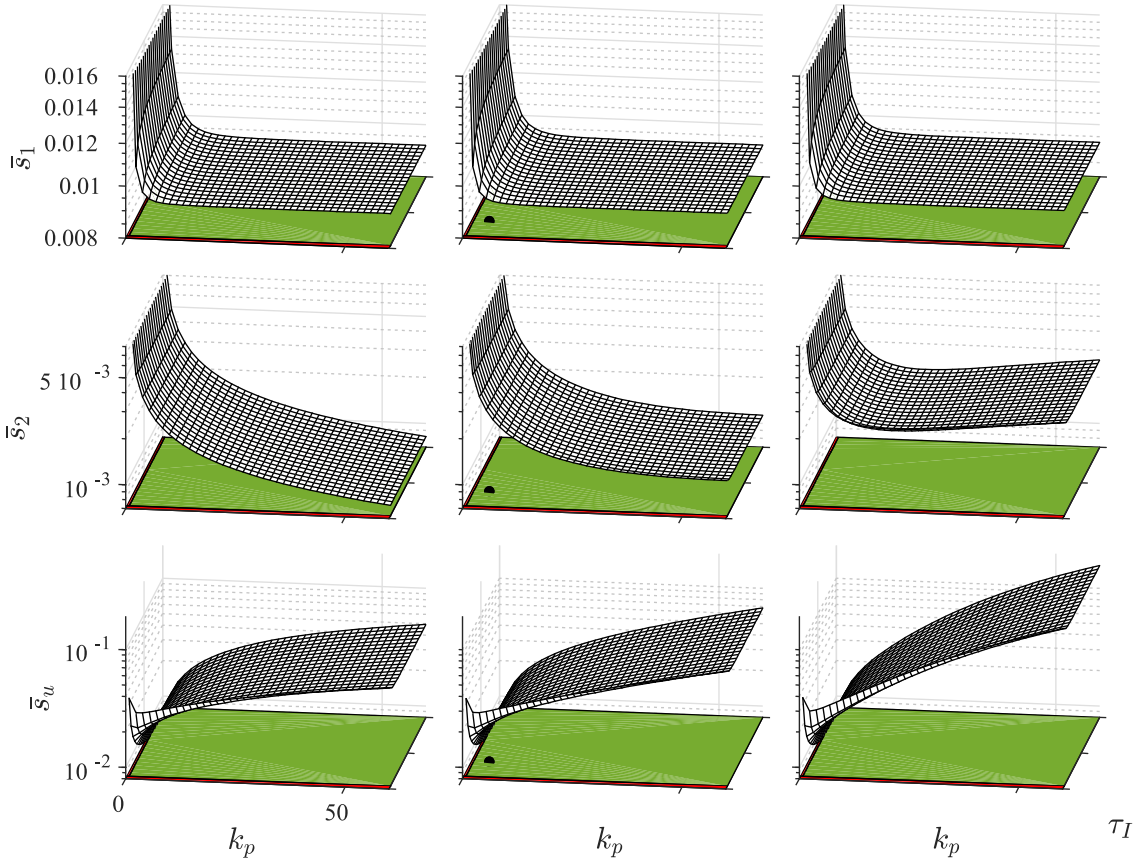


**Fig. 2.** Dependency of the stationary concentration ($\bar{s}_1$) and temperature ($\bar{s}_2$) states as well as control ($\bar{s}_u$) CL state PDF standard deviations on the control gain pair $\boldsymbol{\kappa} \in \mathscr{K}$ (69) for Case $C_1$ (Table 3) with noise STDs (67a-c). • (in bottom plane): tight control gain $\boldsymbol{\kappa}_1^t \in \mathscr{K}_h$ (71a).

variance and skewness than the tight gain $\boldsymbol{\kappa}_1^t$ (71a).

### 6.1.3. CL PDF transient behavior

To assess the CL state PDF (18) transients with tight [$\boldsymbol{\kappa}_1^t$ (71a)] and loose [$\boldsymbol{\kappa}_1^l$ (71b)] control gain pairs: (i) the FP PDE (42) and vector-Riccati ODE (62) systems were set with a +2% change in the mean of the exogenous noise feed temperature disturbance $\boldsymbol{d}_s$ (8f):

$$\boldsymbol{d} = (\bar{\theta}, \bar{x}_{1e}, \bar{x}_{2e} + 0.02)^T \tag{72a}$$

(ii) the FP PDE (42) was set with initial Gaussian PDF $\pi_g$ whose mode $\boldsymbol{x}_{mo}$ is the target one $\bar{\boldsymbol{x}}_m$ (associated to the least probable mode $\bar{z}_m^-$ of the OL bimodal distribution $\bar{\varsigma}(z)$ in Table 3)

$$\pi_o = \pi_g(\boldsymbol{x}),\ \boldsymbol{m}_x(\pi_o) = \bar{\boldsymbol{x}}_m = \bar{\boldsymbol{x}},\ x_{3o} = 0 \tag{72b}$$

and numerically integrated with finite-volume method, and (ii) the vector-Riccati ODE (62) was set with initial zero integral action state and exact initial PDF mode and covariance

$$\widehat{\boldsymbol{x}}_{mo} = \bar{\boldsymbol{x}}_m,\ \widehat{\boldsymbol{\Sigma}}_{mo} = \boldsymbol{\Sigma}_{mo},\ \widehat{x}_{3o} = 0 \tag{72c}$$

and numerically integrated with 4$^{\text{th}}$-order Runge-Kutta method.

The corresponding CL marginal PDFs evolutions (20g), induced by: (i) parasitic concentration, temperature and sensor stochastic noise disturbance and (ii) exogenous mean inlet temperature step disturbance, are presented in Fig. 4, showing that: (i) with the tight gain $\boldsymbol{\kappa}_1^t$ (71a) (left

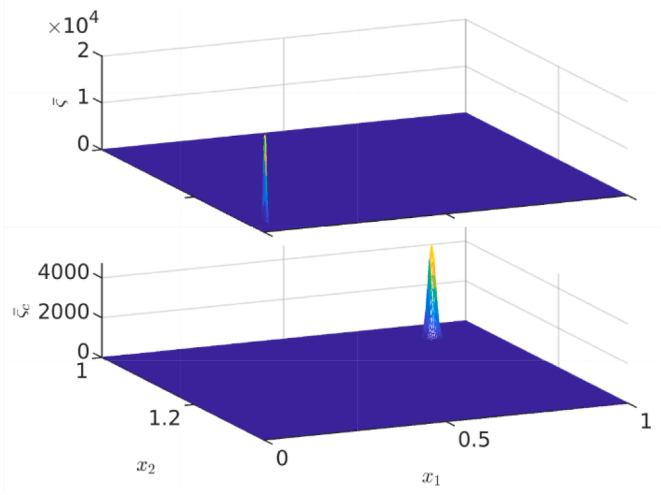


**Fig. 3.** Stationary concentration-temperature state PDFs for Case $C_1$ (Table 3) with tight control gain $\boldsymbol{\kappa}_1^t$ (71a): (i) OL $\bar{\varsigma}(z)$ (11a) (top panel), and (ii) CL marginal $\bar{\varsigma}_c(z)$ (70) (bottom panel) of $\bar{\pi}(\boldsymbol{x})$ (43).

column), the 3-state CL PDF remains monomodal along the entire transient, and (ii) with the loose gain $\boldsymbol{\kappa}_1^l$ (71b) (right column), the PDF becomes bimodal at $t \approx 5$, remains bimodal up to time ≈7, and becomes monomodal thereafter. As expected, in both cases the final state PDF is monomodal. The transient monomodal (or bimodal) behavior manifests the awayness from (or closeness to) of the gain $\boldsymbol{\kappa}_1^t$ (or $\boldsymbol{\kappa}_1^l$) to the boundary $s(\bar{y}, \boldsymbol{\kappa}_i) = 0$ (37b) of the Hurwitz gain set $\mathscr{K}_h$ (69) (where mono-bimodal CL PDF extremum bifurcation occurs, see Fig. 1). The numerical FP PDE-based PDF modeling functions well in close to and away from deterministic bifurcation condition.

From a FP theory modeling perspective (Risken, 1996; Gardiner, 1997), the breakdown of the MC method in close to deterministic bifurcation condition reported in previous OL (Pell and Aris, 1969) and CL (Ratto, 1998) exothermic chemical reactor studies is explained as follows (Alvarez et al., 2018): the PDF characteristics of the infinite-dimensional FP PDE (42) cannot be -in general- captured by the finite-dimensional ODE (26) forced by a sequence of random steps (that approximate the noise $\boldsymbol{w}$).

### 6.1.4. Mode and variance evolutions

In Fig. 5 are presented the actual PDE-based (54) and approximated ODE-based (59) mode transients $\boldsymbol{x}_m$ and $\widehat{\boldsymbol{x}}_m$, respectively, with tight [$\boldsymbol{\kappa}_1^t$ (71a)] and loose [$\boldsymbol{\kappa}_1^l$ (71b)] control gain pairs and input-initial condition (72), showing that: (i) with $\boldsymbol{\kappa}_1^t$, $\boldsymbol{x}_m$ (left column) evolves over almost deterministic time scale $t_x \approx 5$, and $\widehat{\boldsymbol{x}}_m$ (left column) $\varepsilon$-P converges (61) (with imperceptible to the eye error) to $\boldsymbol{x}_m$, and (ii) with $\boldsymbol{\kappa}_1^l$, $\boldsymbol{x}_m$ (right column) evolves over deterministic-diffusion time biscale $t_\pi \approx 25$, and $\widehat{\boldsymbol{x}}_m$ (right column) $\varepsilon$-P converges (61) (with admissible transient error) or not (if the error size is inadmissible) to $\boldsymbol{x}_m$, depending on the specific reactor and operation condition in actual variables and dimensions and associate model parameter uncertainties. In agreement with Proposition 9, in both gain cases, the approximated versus actual asymptotic mode error is zero.

In Fig. 6 are presented the actual CL FP PDE-based (42) (left panel) and approximated CL Riccati ODE-based (62a-b) (right panel) state [$\mu_{x_i}$ (20g)] and control [$\nu$ (20f)] marginal PDFs evolutions in contour form (yellow/blue curve: most/least probable value) along with the mode evolutions for the tight gain case $\boldsymbol{\kappa}_1^t$, showing (in agreement with results of Section 5.2 and of Fig. 5) that: (i) the actual marginal state ($\mu_{x_i}$) and control ($\nu$) CL PDFs evolve over almost deterministic time scale $t_x \approx 5$, and the approximated ones $\widehat{\mu}_{x_i}$ and $\widehat{\nu}$ (bottom panels) $\varepsilon$-P converge (61) (with imperceptible to the eye error) to $\mu_{x_i}$ and $\nu$. The agreement

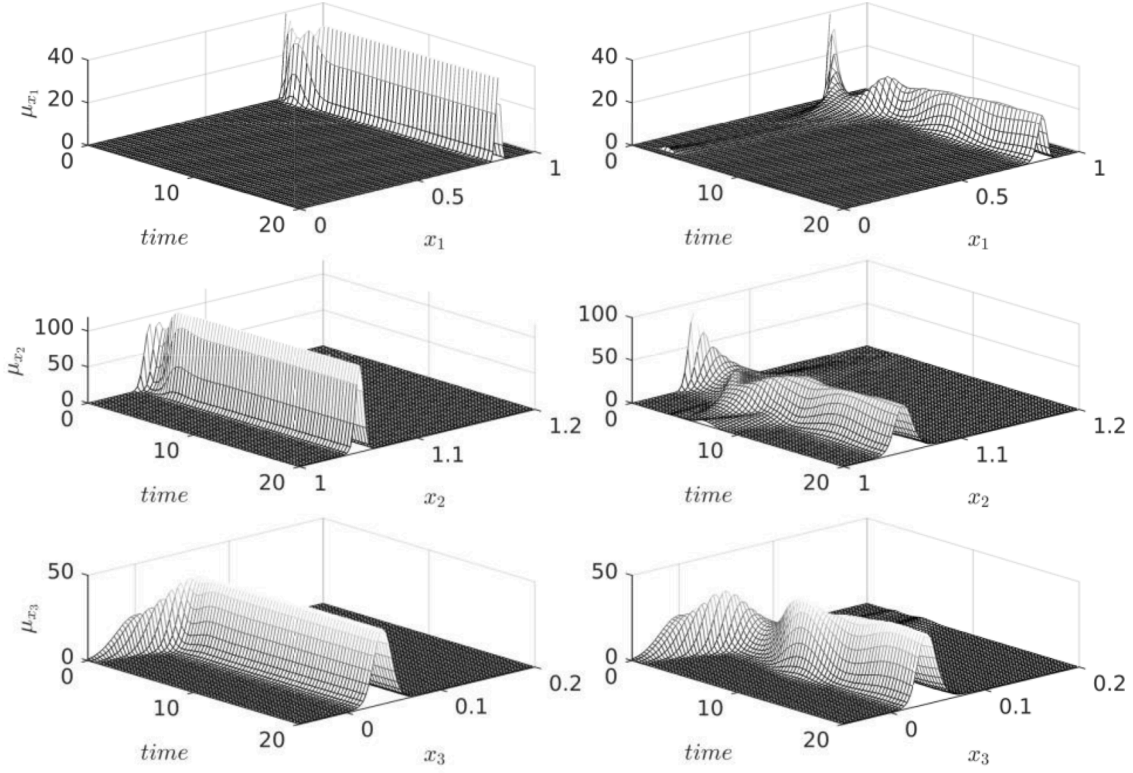


**Fig. 4.** For Case $C_1$ (Table 3) with tight (71a) (left panel) [or loose (71a) (right panel] control gain $\boldsymbol{\kappa}_1^t$ (or $\boldsymbol{\kappa}_1^l$) $\in \mathscr{K}_h$, exogenous noise with mean feed temperature step disturbance $\boldsymbol{d}$ (72a), and noise STD (67), CL evolutions of: (i) FP PDE (42)-based marginal concentration ($\mu_{x_1}$), temperature ($\mu_{x_2}$), and integral action ($\mu_{x_3}$) state (20g) 1D PDFs.

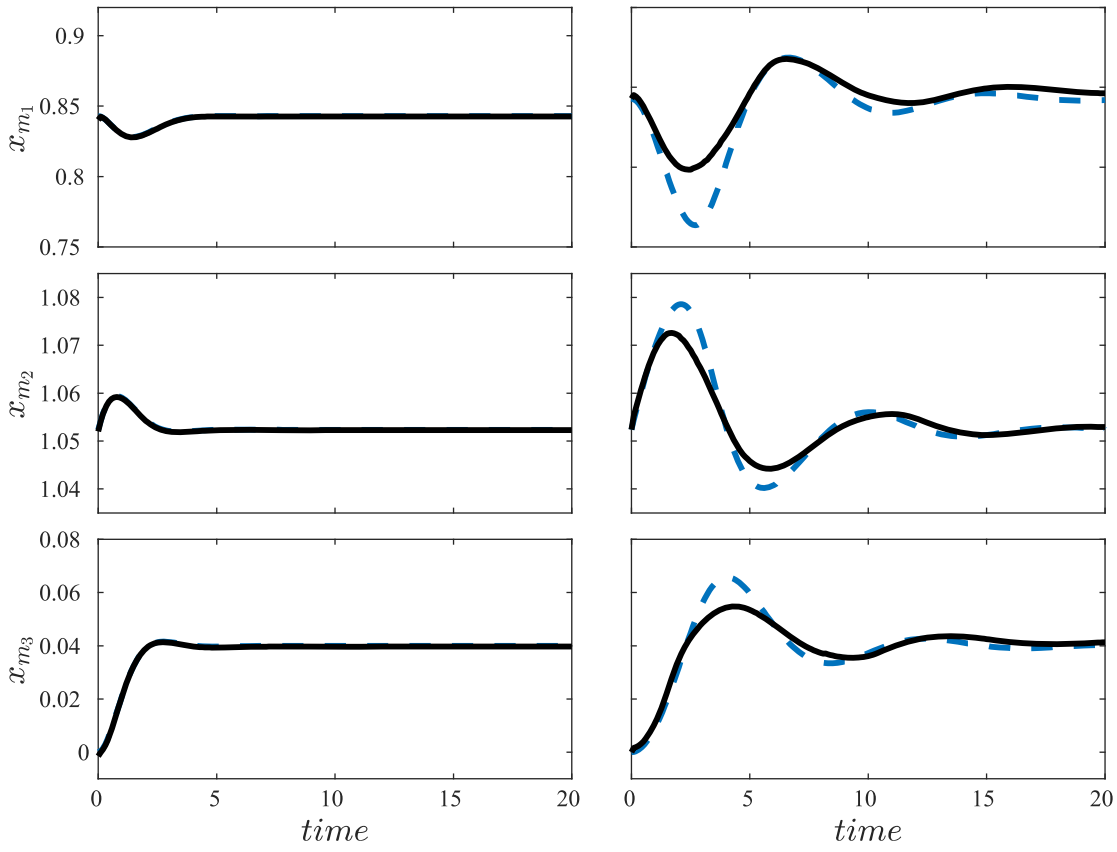


**Fig. 5.** For Case $C_1$ (Table 3) with tight (71a) (left panel) [or loose (71a) (right panel)] control gain $\boldsymbol{\kappa}_1^t$ (or $\boldsymbol{\kappa}_1^l$) $\in \mathscr{K}_h$, exogenous noise with mean feed temperature step disturbance $\boldsymbol{d}$ (72a), and noise STD (67), CL evolutions of: (i) FP PDE (54) (black continuous curves) and Riccati ODE (62a) (discontinuous blue curves)-based concentration ($x_{m1}$), temperature ($x_{m2}$), and integral action ($x_{m3}$) state modes (20b).

between CL Riccati-based (left panel) and numerical solution of the CL FP PDE (right panel) marginals is rather good at any time since the enhanced-by-feedback CL diffusion characteristic time scale is comparable to the deterministic one. This verifies the methodological proposal (Section 5.2) of selecting the control gain with a two-step procedure: gross tuning with the Hurwitz criterion [(37) and (69)] in the light of stationary state and control STDs (68) followed by fine tuning with stationary and transient FP PDE simulation.

The preceding results and discussion confirm and illustrate the theoretical development presented in Sections 4-5. With CL FP PDE (42) simulation: (i) in Figs. 4 to 6, the transient associated with the state PDF RM stability property (25) has been displayed, and (ii) in Fig. 5, the $\epsilon$-P mode convergence property (61) has been validated.

### 6.1.5. Random state motions

Here, the preceding FP PDE-based results are corroborated and illustrated with the MC-type simulation employed in previous stochastic dynamics (Pell and Aris, 1969; Doraiswamy and Kulkarny, 1986; Ratto, 1998) and IS stability (Wu et al., 2018a,b; Lu et al., 2022) reactor studies.

Following the MC SDE simulation schemes employed in previous studies on CL stochastic with linear PI (Ratto, 1998) and NL passive (Wu et al., 2018a,b; Lu et al., 2022) control in the light of industrial protocol testing schemes (Franco-de los Reyes and Alvarez, 2022), let us integrate the SDE (15), with Euler-Maruyama method (Kloeden and Platen, 1992) and time step $1 \times 10^{-4}$, subjected to parasitic and instrument measurement noise disturbance with standard deviations $\sigma_i$ (67) and mean value step change $\boldsymbol{d}_1$ (or $\boldsymbol{d}_2$) in exogenous stochastic feed concentration (or temperature) disturbance $\boldsymbol{d}_{s1}$ (or $\boldsymbol{d}_{s2}$) (8f):

$$\boldsymbol{d}_1 = (\bar{\theta}, \bar{x}_{1e} + 0.05, \bar{x}_{2e})^T, \ \boldsymbol{d}_2 = (\bar{\theta}, \bar{x}_{1e}, \bar{x}_{2e} - 0.02)^T \quad (73ab)$$

In Fig. 7 are presented the resulting CL SDE (15)-based Brownian random state motions $\boldsymbol{x}(t)$ (16) (blue and red noisy curves), accompanied -for comparison purposes- by the corresponding CL FP PDE (42)-based state PDF evolution $\pi(\boldsymbol{x}, t)$ (18), for exogenous disturbance $\boldsymbol{d}_1$ with tight control gain $\boldsymbol{\kappa}_1^t \in \mathscr{K}_h$ (71a). In agreement with the theoretical developments of Sections 3 to 5 and industrial control practice: (i) the temperature random motions (second panel) have zero-mode asymptotic offset, and (ii) the concentration (first panel) and integral (third panel) random motions have mode asymptotic offset, (iii) the control input (fourth panel) has mode asymptotic offset. The variability of state and control motions are within the region delimitated by the marginal state (20g) and control (20f) PDFs (see Fig. 7) that encompass all possible Brownian random motions. The state and control mode and their variabilities reach stationary behavior along almost deterministic time scale, in agreement with the $\epsilon$-P convergence result (61) of Section 5.2.

In Fig. 8 are presented the resulting Brownian random state motions (blue and red noisy curves) for exogenous disturbance $\boldsymbol{d}_2$ (73b) with tight control gain $\boldsymbol{\kappa}_1^t \in \mathscr{K}_h$ (71a). While the same conclusion of the previous case for variability and characteristic time scale can be drawn, in this case according with industrial control practice: (i) the concentration (first panel) and the temperature random motions (second panel) have zero-mean asymptotic offset, and (ii) the integral (third panel) and the control input (fourth panel) random motions have mean asymptotic offset.

The FP PDE (42)-based state PDF motion $\pi(\boldsymbol{x}, t)$ (18) and SDE (15)-based random motion $\boldsymbol{x}(t)$ (16) simulation results of Figs. 7 and 8 agree with and confirm the theoretical developments and results of Sections 3 to 5 on: (i) state PDF RM stability (25), (ii) and random state motion R IP $\bar{\boldsymbol{x}}$-stability (53) in the light of state PDF RM stability (25), and (ii) and illustrates graphically why state PDF RM $\bar{\pi}$-stability implies R IP

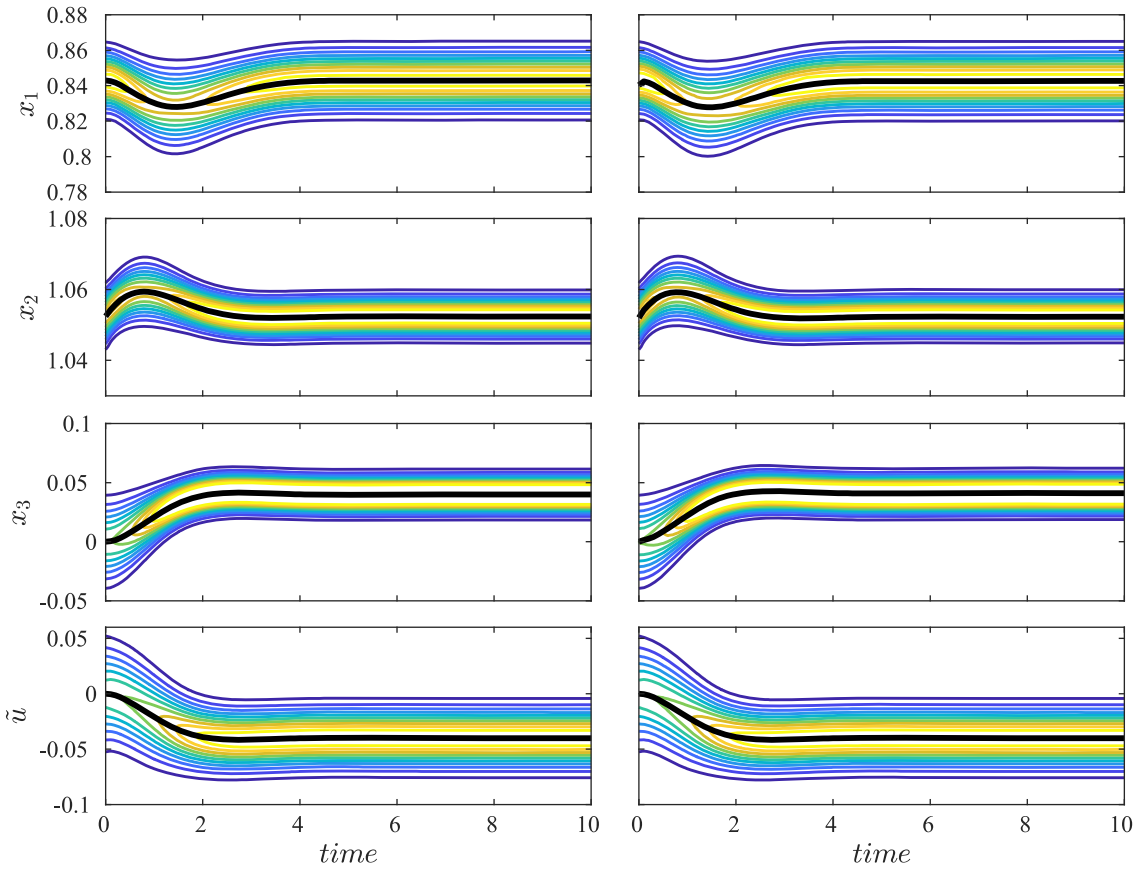


**Fig. 6.** For Case $C_1$ (Table 3) with tight control gain $\boldsymbol{\kappa}_1^t \in \mathscr{K}_h$ (70a), exogenous noise with mean feed temperature step disturbance $\boldsymbol{d}$ (71a), and noise STD (67), CL evolutions of: (i) FP PDE (42) (left panel) and Riccati ODE (62) (right panel) -based marginal concentration ($\mu_{x_1}$), temperature ($\mu_{x_2}$), and integral action ($\mu_{x_3}$) state (20g) as well as control ($\nu$) (20f) PDFs in contour form, and state and control modes (20b) (continuous black curve).

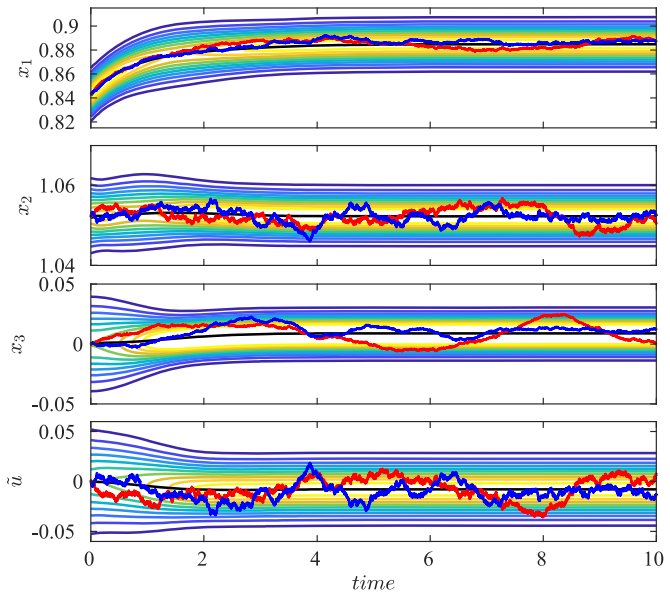


**Fig. 7.** For Case $C_1$ (Table 3) with tight control gain $\boldsymbol{\kappa}_1^t \in \mathscr{K}_h$ (71a), exogenous noise with mean feed composition step disturbance $\boldsymbol{d}_1$ (73a), and noise STD (67), CL evolutions of SDE (15)-based random state motions and control (16) (red and blue noisy curves), and (ii) for comparison, FP PDE (42)-based marginal concentration ($\mu_{x_1}$), temperature ($\mu_{x_2}$), and integral action ($\mu_{x_3}$) state (20g) and control ($\nu$) (20f) PDF in contour form, as well as state and control modes (20b) (continuous black curve).

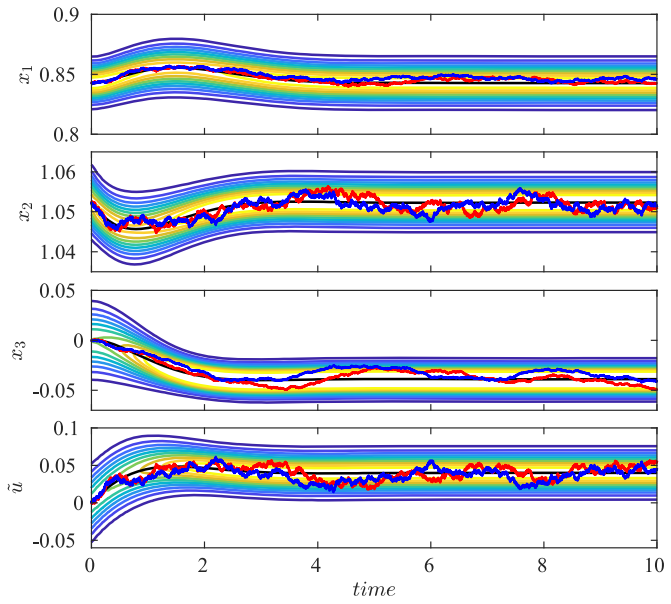


**Fig. 8.** For Case $C_1$ (Table 3) with tight control gain $\boldsymbol{\kappa}_1^t \in \mathscr{K}_h$ (71a), exogenous noise with mean feed temperature step disturbance $\boldsymbol{d}_2$ (73b), and noise STD (67), CL evolutions of SDE (15)-based random state motions and control (16) (red and blue noisy curves), and (ii) for comparison, FP PDE (42)-based marginal concentration ($\mu_{x_1}$), temperature ($\mu_{x_2}$), and integral action ($\mu_{x_3}$) state (20g) and control ($\nu$) (20f) PDF in contour form, as well as state and control modes (20b) (continuous black curve).

$\bar{x}$-stability.

Since the PDF evolution (18) of the FP PDE (42) contains the complete statistical information on the entire random motion bundle set (16) of the SDE (15), the obtainment with MC method of same kind of global [over the entire probability state space $\mathscr{X}$ (15c)] description is a rather complex specialized task that requires a sufficiently large random motion sample with PDF shape model selection (Vesterinen and Ritala, 2005).

### 6.2. Case $C_2$ (OL robust bimodal PDF)

In case $C_2$ (Fig. 1, Table 3): (i) the OL 2-state state PDF is robustly equiprobable bimodal, and (ii) the controller must attain R 3-state CL monomodality with most probable state at the almost null probable OL saddle.

In Fig. 9, the analytic dependency on the gain $\boldsymbol{\kappa} \in \mathscr{K}_h$ (69) (green subset of the bottom gain plane $\mathscr{K}$) of the stationary concentration and temperature state as well as control STDs on gains for background noise intensity (67) are presented. The concentration STD (top panel) decreases with the proportional gain, reaching an asymptotic value determined by the background noise and temperature measurement noise STDs. The temperature STD (central panel) initially decreases with proportional, reaches a minimum, and grows thereafter. The control STD stand (bottom panel) initially decreases with proportional gain, reaches a minimum, and grow thereafter. As expected, the decrease of rest time (increase of integral gain) increases noise-to-control STD propagation.

On the basis of the analytic (Appendix D) state and control standard deviation dependencies on the gain pair $\boldsymbol{\kappa}$ plotted in Fig. 9 plus FP PDE simulation-based tuning, the control gain pair (dot in the bottom plane of Fig. 9)

$$\boldsymbol{\kappa}_2 = \left(k_p, \tau_I\right)^T = (8, 1)^T \in \mathscr{K}_h \tag{74}$$

was chosen to get an adequate compromise between regulation speed, state and control effort modes and variances.

The resulting CL robust concentration-temperature marginal PDF $\bar{\varsigma}_c$ (70) is plotted in Fig. 10 (bottom panel). In the open-to-closed loop passage the PDF saddle (associated to the unstable deterministic steady state) becomes the most probable state of a monomodal state PDF, in agreement with Proposition 5.

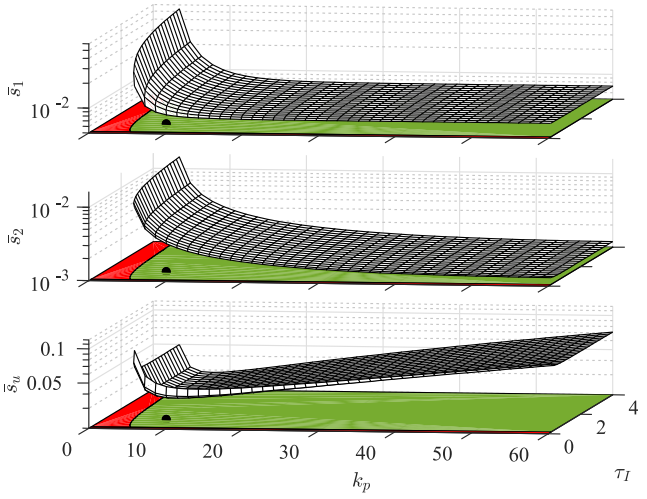


**Fig. 9.** Dependency of the CL stationary concentration ($\bar{s}_1$) and temperature ($\bar{s}_2$) states as well as control ($\bar{s}_u$) PDF STDs on the control gain pair $\boldsymbol{\kappa} \in \mathscr{K}_h$ (69) for Case $C_2$ (Table 3) with noise STDs (67). • (in bottom plane $\mathscr{K}$): control gain $\boldsymbol{\kappa}_2 \in \mathscr{K}_h$ (74).

### 6.3. Case $C_3$ (OL robust vulcanoid PDF)

In case $C_3$ (Fig. 1, Table 3): (i) the OL 2-state state PDF has vulcanoid shape, and (ii) the controller must attain R 3-state CL monomodality with most probable state at the almost null probable OL volcano bottom.

In Fig. 11, the analytic dependencies on the gain $\boldsymbol{\kappa} \in \mathscr{K}_h$ (69) (green subset of the bottom gain plane $\mathscr{K}$) of the stationary concentration and temperature state as well as control STDs on control gain are plotted for the noise STDs (67). The STD on gain dependency is similar to the one (Fig. 2) of Case $C_1$, with an important difference: the temperature STD exhibits a more pronounced minimum (at gain $k_p \approx 12$). This reflects the fact that the temperature set point of the PI control is associated with: (i) the absolute minimum (bottom point) of the OL vulcanoid PDF, and (ii) the unstable focus of the deterministic limit cycle.

On the basis of the analytic (Appendix D) state and control standard deviation dependencies on the gain pair $\boldsymbol{\kappa}$ plotted in Fig. 11 followed by some FP PDE simulation-based tuning, the control gain pair (dot in the bottom plane of Fig. 11)

$$\boldsymbol{\kappa}_3 = \left(k_p, \tau_I\right)^T = (4, 1)^T \in \mathscr{K}_h \tag{75}$$

was chosen to attain an adequate compromise between regulation speed, state and control effort variances.

The resulting CL stationary concentration-temperature marginal PDF $\bar{\varsigma}_c$ (70) is presented in Fig. 12 (bottom panel), confirming again that -in agreement with theoretical results- in the open-to-closed loop passage the almost improbable vulcanoid PDF bottom tip (associated with the center of a deterministic OL LC) becomes the most probable state of a monomodal state PDF.

## 7. Conclusions

The longstanding problem (Ratto, 1998; Ratto and Paladino, 2000) of assessing the CL stochastic dynamics of a class (15) of 2-state NL exothermic continuous reactors with complex OL dynamics, PI temperature control, and combined random noise-deterministic load disturbance has been formally resolved by characterizing the CL state PDF dynamics with Fokker Planck (FP) theory.

The dependency of the stochastic CL state PDF dynamics on deterministic global dynamics was established, including the geometric correspondence between stationary state PDF and deterministic global monostability. This dependency is important to exploit the accumulated knowledge and insight on deterministic reactor NL dynamics in the

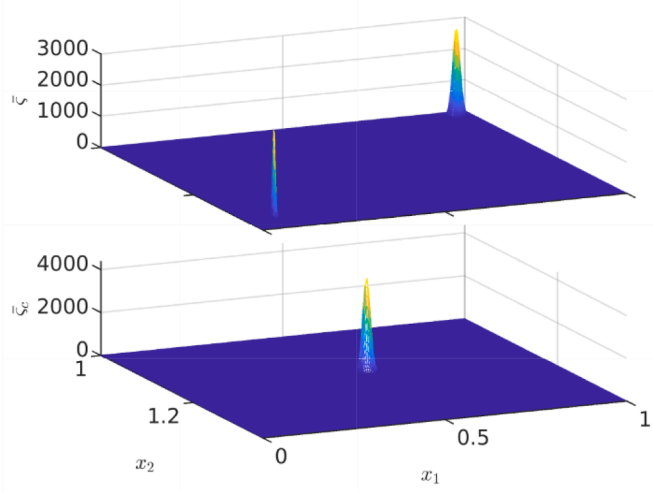


**Fig. 10.** Stationary concentration-temperature state PDFs for Case $C_2$ (Table 3) with control gain $\boldsymbol{\kappa}_2 \in \mathscr{K}_h$ (74): (i) OL $\bar{\varsigma}(z)$ (11a) (top panel), and (ii) CL marginal $\bar{\varsigma}_c(z)$ (70) (bottom panel) of $\bar{\pi}(\boldsymbol{x})$ (43).

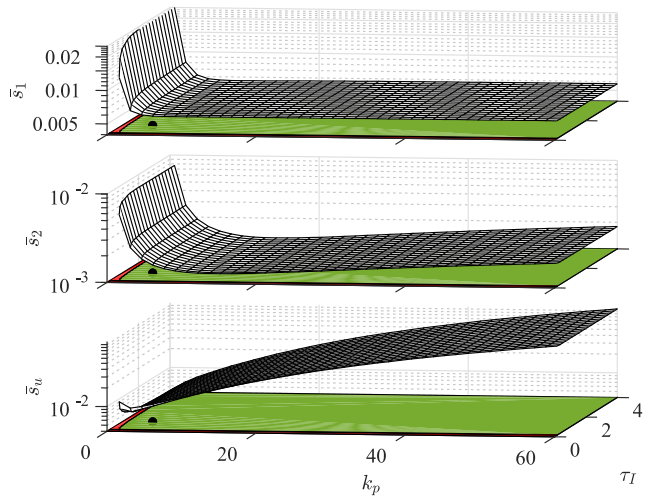


**Fig. 11.** Dependency of the CL stationary concentration ($\bar{s}_1$) and temperature ($\bar{s}_2$) states as well as control ($\bar{s}_u$) PDF STDs on the control gain pair $\boldsymbol{\kappa} \in \mathscr{K}_h$ (69) for Case $C_3$ (Table 3) with noise STDs (67). • (in bottom plane $\mathscr{K}$): control gain $\boldsymbol{\kappa}_3 \in \mathscr{K}_h$ (75).

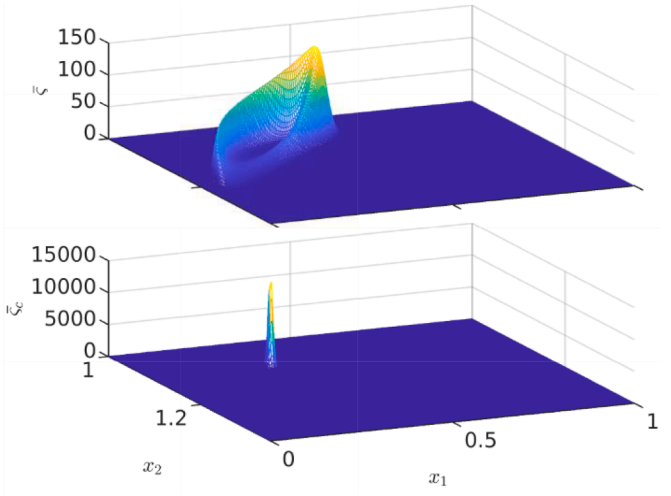


**Fig. 12.** Stationary concentration-temperature state PDFs for Case $C_3$ (Table 3) with control gain $\boldsymbol{\kappa}_3$ (75): (i) OL $\bar{\varsigma}(z)$ (11a) (top panel), and (ii) CL marginal $\bar{\varsigma}_c(z)$ (70) (bottom panel) of $\bar{\pi}(\boldsymbol{x})$ (43).

stochastic dynamics assessment and PI control tuning tasks. It was shown that the definition of R PDF stability employed in this study implies the R(EUB) generalization of the definition of IP stability employed in previous stochastic reactor control studies with NL SF economic model predictive (Wu et al 2018a,b) and passive (Lu et al., 2022) control. Along pioneering studies with local FP and MC method (Ratto, 1998; Ratto and Paladino, 2000) and current industrial trends (Samad, 2017; Maxim et al., 2019), a further step towards the development of a FP theory-based joint PI-SP control design methodology for industrial reactors with complex OL PDF dynamics has been taken.

It was formally established that: (i) stochastic state PDF RM stability requires deterministic global R stability, which in turn requires deterministic passivity and adequate control gain, (ii) the CL RM stable state PDF motions evolve, without metastability, along deterministic and probability diffusion time scales, (iii) with a proper control gain the most probable (MP) state and control and their variabilities evolve along almost deterministic time scale (an interesting and relevant application-oriented property for joint PI-SP control scheme analysis and development). It was concluded that, from a FP modeling perspective: (i) the industrial PI control regulates the reactor MP state by adjusting the MP control on the basis of the MP temperature measurement, (ii) the proportional action ensures state PDF RM stability, and (iii) the integral action enables MP temperature (or concentration) asymptotic mode offset elimination (or attenuation) with respect to persistent deterministic and/or not zero-mean stochastic disturbances. The interplay between gain choice, state PDF regulation capability, and control effort in a stochastic sense was identified. An application-oriented efficient two-step gain tuning scheme was proposed: analytic formulae-based gross tuning followed by FP PDE simulation-based fine tuning.

The proposed methodology was illustrated and tested with three indicative examples with OL complex (bimodal and vulcanoid, and metastability) state PDF dynamics. With FP PDE numerical simulation for the examples, it was corroborated that: (i) CL RM monomodality is achieved, and (ii) the proposed methodology functions well in away from and close to deterministic bifurcation, while the MC method of previous OL (Pell and Aris, 1969) and CL (Ratto, 1998) reactor studies breaks down in close to deterministic bifurcation. With MC-type CL SDE simulation, it was verified and illustrated: (i) random state motion IP stability in the light of state PDF RM stability, and (ii) random motion-control behavior in the presence of combined random endogenous zero-mean and exogenous time-varying noise disturbances.

The present study is a point of departure to address in the future: (i) the optimization-based systematization of PI control gain tuning in the light of SP control, (ii) the compensation of PDF extremum shifting due to multiplicative noise (Krstic and Deng, 1988; Baratti et al., 2018), (iii) the development of the observer-based MP state control variant of the stochastic passive NL mean SF IP stabilizing control (Krstic and Deng, 1988; Wu et al., 2018a,b; Lu et al., 2022), (iv) the supplementation of the proposed PI control-based MP state regulation scheme with a non-interfering MP state estimator for setpoint adjustment in a supervisory layer (McAvoy, 2002; Maxim et al., 2019), and (v) the deterministic-to-stochastic extension of the saturated PI control with anti-windup protector (Alvarez et al., 1991; Schaum et al., 2012; Franco-de los Reyes and Alvarez, 2022).

## CRediT authorship contribution statement

**Jesus Alvarez:** Conceptualization, Methodology, Writing – review & editing. **Roberto Baratti:** Conceptualization, Methodology, Software, Visualization, Writing – original draft.

## Declaration of Competing Interest

The authors declare that they have no known competing financial interests or personal relationships that could have appeared to influence the work reported in this paper.

## Appendix A. Hurwitz conditions for deterministic SS stability

The 3 × 3 Jacobian matrix of the deterministic system (26) at its prescribed SS $\bar{\boldsymbol{x}} =$ (35) is

$$\bar{\boldsymbol{J}} = \left[\boldsymbol{L}(\bar{y}, k_p)\boldsymbol{v}\boldsymbol{h}(k_I)0\right],\ \bar{\boldsymbol{J}} = \boldsymbol{J}(\bar{\boldsymbol{x}}),\ \boldsymbol{J}(\boldsymbol{x}) = [\partial_{\boldsymbol{x}}\boldsymbol{f}(\boldsymbol{x}, \bar{\boldsymbol{d}}, \boldsymbol{k})],\ \boldsymbol{f}:\ (34) \tag{A1a}$$

where

$$\boldsymbol{L}(\bar{y}, k_p) = \left[-l_1(\bar{y})\ -c_1(\bar{y})c_2(\bar{y}) - l_2(\bar{z}, k_p)\right],\ \boldsymbol{v} = \begin{bmatrix} 0 \\ -\eta \end{bmatrix},\ \boldsymbol{h}(k_I) = [0,\ k_I]$$

$$c_1 = (\delta/2)r_1(\bar{y}),\ c_2 = (\delta/2)r_2(\bar{y}),\ r_i(\bar{y}) = [\partial_{x_i} r(x_1, x_2)]_{x_1 = m(\bar{y}), x_2 = \bar{y}}$$

$$l_1(\bar{y}, k_p) = \bar{\theta} + \delta r_1(\bar{y}),\ l_2(\bar{y}, k_p) = l_{2o}(\bar{\boldsymbol{x}}) + \eta k_p,\ l_{2o}(\bar{y}, k_p) = \bar{\theta} + \eta - \frac{\delta}{2} r_2(\bar{y})$$

The characteristic polynomial of $\bar{\boldsymbol{J}}$ (A1) is

$$\lambda^3 + a_1(\bar{y}, k_p)\lambda^2 + a_2(\bar{y}, k_p)\lambda + a_3(\bar{y}, k_I) = 0 \tag{A2a}$$

where

$$a_1(\bar{y}, k_p) = T_{\boldsymbol{L}}(\bar{y}, k_p),\ a_2(\bar{y}, k_p) = D_{\boldsymbol{L}}(\bar{y}, k_p) + k_I\eta,\ a_3(\bar{y}, k_I) = k_I\eta l_1 \tag{A2bd}$$

$$T_{\boldsymbol{L}}(\bar{y}, k_p) = l_1(\bar{y}) + l_2(k_p),\ D_{\boldsymbol{L}}(\bar{y}, k_p) = l_1(\bar{y}, k_p)l_2(k_p) + c(\bar{y}),\ c(\bar{y}) = \frac{\delta^2}{2} r_1(\bar{y})r_2(\bar{y}) \tag{A2eg}$$

The Hurwitz stability conditions (37b) of Proposition 2 are (Boyce and Di Prima, 1967)

$$s_1 = a_1,\ s_2 = a_1a_2 - a_3,\ s_3 = a_3 \tag{A3ac}$$

or in detailed form

$$s_1(\bar{y}, k_p) = T_{\boldsymbol{L}}(\bar{y}, k_p),\ s_2(\bar{y}, k_I) = k_I\eta l_1(\bar{y}),\ s_3(\bar{y}, \boldsymbol{k}) = T_{\boldsymbol{L}}(\bar{y}, k_p)D_{\boldsymbol{L}}(\bar{y}, k_p) + l_2(\bar{y}, k_p)\eta k_I \tag{A4ac}$$

## Appendix B. Proof of Proposition 8 (*State mode rate of change*)

Following (Jazwinski, 1970), the time derivation of the null-gradient condition (20b) followed by substitution of the RHS of the FP PDE (41) yields that the state mode rate of change is given by

$$\dot{\boldsymbol{x}}_m = -\left[(\boldsymbol{H}\pi)^{-1}\nabla\mathscr{F}\right]_{\boldsymbol{x}=\boldsymbol{x}_m},\ \mathscr{F}:\ (19a),\ \nabla,\ \boldsymbol{H}:\ (20e) \tag{B1}$$

The application of the vector analysis formula (Oates, 1974) (for the divergency of the vector-scalar field product $\boldsymbol{v}\pi$)

$$\nabla\cdot(\boldsymbol{v}\pi) = (\nabla\pi)\cdot\boldsymbol{v} + (\nabla\cdot\boldsymbol{v})\pi$$

to the probability transport-generation operator $\mathscr{F}$ of the FP PDE (41) yields the gradient of $\mathscr{F}$

$$\nabla\mathscr{F} = \nabla[\nabla\cdot((1/2)\boldsymbol{Q}\nabla\pi)] - (\mathscr{H}\pi)\boldsymbol{f} - \left[\boldsymbol{J}^T + \boldsymbol{I}(\nabla\cdot\boldsymbol{f})\right]\nabla\pi\ - [\nabla(\nabla\cdot\boldsymbol{f})]\pi,\ \boldsymbol{Q}:(14h),\ \boldsymbol{J}:\ (A1a)$$

which at the state mode $\boldsymbol{x}_m$ (where $\nabla\pi = 0$) becomes

$$\nabla\mathscr{F}(\pi,\ \boldsymbol{d}) = \nabla[(1/2)\nabla\cdot(\boldsymbol{Q}\nabla\pi)] - (\mathscr{H}\pi)\boldsymbol{f} - [\nabla(\nabla\cdot\boldsymbol{f})]\pi$$

The substitution of this expression in (B1) followed by arrangement yields the FP PDE-based mode rate of change (56) of Proposition 8. **QED**

## Appendix C. Proof of Proposition 9 (*Mode evolution*)

By the CL deterministic stability property (40), the state [$\widetilde{\boldsymbol{x}}_m$: (C1a)] and control [$\widetilde{u}_m$: (C2b)] mode and control evolution deviations of the PDF-dependent ODE system (56) with $\boldsymbol{d} = \bar{\boldsymbol{d}}$ and $\varrho_\pi = 0$

$$\dot{\boldsymbol{x}}_m = \boldsymbol{f}(\boldsymbol{x}_m, \bar{\boldsymbol{d}}),\ \boldsymbol{x}_m(0) = \boldsymbol{x}_{mo} = \boldsymbol{m}_x(\pi_o)$$

are bounded by

$$|\widetilde{\boldsymbol{x}}_m(t)| \le a_x e^{-\lambda_x t}|\widetilde{\boldsymbol{x}}_{mo}|^+ := s(t),\ \widetilde{\boldsymbol{x}}_m := \boldsymbol{x}_m(t) - \bar{\boldsymbol{x}} \tag{C1a}$$

$$|\widetilde{u}_m(t)| \le k_{\boldsymbol{x}_m}^{\boldsymbol{c}_u} a_x e^{-\lambda_x t}|\widetilde{\boldsymbol{x}}_{mo}|^+,\ \widetilde{u}_m = u_m(t) - \bar{u} \tag{C1b}$$

or equivalently, by the linear scalar ODE-based form

$$|\widetilde{\boldsymbol{x}}_m(t)| \le s(t):\ \dot{s} = -\lambda_x s,\ s_o(0) = s_o = a_x|\widetilde{\boldsymbol{x}}_{mo}|^+,\ |\widetilde{u}_m(t)| \le k_{\boldsymbol{x}_m}^{\boldsymbol{c}_u} s(t) \tag{C2}$$

From the application (Gonzalez and Alvarez, 2005, Franco-de los Reyes and Alvarez, 2022) of Lyapunov's Converse Theorem (Vidyasagar, 1993) to (56a) in the light of (C1) and (C2), the mode and control evolution deviations of the PDF-dependent ODE system (56) are bounded as

$$|\widetilde{\boldsymbol{x}}_m(t)| \le s(t):\ \dot{s} = -\left(\lambda_x - a_x l_{\boldsymbol{x}_m}^{e_\pi}\right)s + (a_x/\lambda_x)l_{\boldsymbol{d}}^{f}|\widetilde{\boldsymbol{d}}|^{+}:\ \boldsymbol{s}_o(0) = s_o \tag{C3a}$$

$$|\widetilde{u}_m(t)| \le k_{\boldsymbol{x}_m}^{e_u} s(t),\ s_o = a_x|\widetilde{\boldsymbol{x}}_{mo}|^{+},\ \lambda_x > a_x l_{\boldsymbol{x}_m}^{e_\pi},\ l_{\boldsymbol{x}_m}^{e_\pi}:\ (55b),\ l_{\boldsymbol{d}}^{f}:\ (39d) \tag{C3b}$$

From the analytic integration of the linear ODE (C3a) the algebraic bounding inequalities (58) of Proposition 9 follow. **QED**

## Appendix D. Stationary state covariance and control variance

### D.1. State covariance matrix

In terms of the proportional-integral gain vector $\boldsymbol{k}$ (12), the analytic solution of the stationary Riccati equation (64e) with $\bar{\Sigma} = \bar{\Sigma}_m$ (64b) is given by the state covariance matrix

$$\bar{\Sigma}_m(\boldsymbol{k}) = \begin{bmatrix} \bar{\sigma}_{11} & \bar{\sigma}_{12} & \bar{\sigma}_{13} \\ \bar{\sigma}_{12} & \bar{\sigma}_{22} & \bar{\sigma}_{23} \\ \bar{\sigma}_{13} & \bar{\sigma}_{23} & \bar{\sigma}_{33} \end{bmatrix} = \bar{\Sigma}(\boldsymbol{k}),\ \boldsymbol{k} \in K_h \subset K,\ K:\ (12c),\ K_h:\ (37) \tag{D1}$$

where

$$\bar{\sigma}_{11}(\boldsymbol{k}) = \frac{k_I\left[2\eta k_I \bar{l}_2(k_p) + 2\bar{l}_2(k_p)^2\bar{l}_1 + 2\bar{l}_2(k_p)\bar{l}_1^2 + \delta^2\bar{l}_1\bar{r}_{x_1}\bar{r}_{x_2}\right]q_1 + 2\delta^2 k_I\bar{l}_1\bar{r}_{x_2}^2 q_2 + 2\delta^2\eta\bar{r}_{x_2}^2\left(\bar{l}_2(k_p) + \bar{l}_1\right)q_3}{2k_I\bar{l}_1 L_d(\boldsymbol{k})} \tag{D2a}$$

$$\bar{\sigma}_{12}(\boldsymbol{k}) = \frac{\delta k_I\bar{l}_2(k_p)\bar{r}_{x_1}q_1 + 2\delta k_I\bar{l}_1\bar{r}_{x_2}q_2 - 2\delta\eta\bar{r}_{x_2}\left(\bar{l}_2(k_p) + \bar{l}_1\right)q_3}{2k_I L_d(\boldsymbol{k})} \tag{D2b}$$

$$\bar{\sigma}_{13}(\boldsymbol{k}) = \frac{\delta k_I^2\bar{l}_2(k_p)\bar{r}_{x_1}q_1 - 2\delta k_I^2\bar{l}_1\bar{r}_{x_2}q_2 + \delta\left[\bar{r}_{x_2}\left(\bar{l}_2(k_p) + \bar{l}_1\right)\left(2\bar{l}_2(k_p)\bar{l}_1 + \delta^2\bar{r}_{x_1}\bar{r}_{x_2}\right) - 2\eta k_I\bar{l}_1\bar{r}_{x_2}\right]q_3}{2k_I\bar{l}_1 L_d(\boldsymbol{k})} \tag{D2c}$$

$$\bar{\sigma}_{22}(\boldsymbol{k}) = \frac{\delta^2 k_I\bar{r}_{x_1}^2 q_1 + 2k_I\left[2\eta k_I + 2\bar{l}_2(k_p)\bar{l}_1 + 2\bar{l}_1^2 + \delta^2\bar{r}_{x_1}\bar{r}_{x_2}\right]q_2 + 4\left[\eta^2 k_I + \eta\bar{l}_2(k_p)\bar{l}_1 + \eta\bar{l}_1^2\right]q_3}{4k_I L_d(\boldsymbol{k})} \tag{D2d}$$

$$\bar{\sigma}_{23}(\boldsymbol{k}) = -\tfrac{q_3}{2k_I},\ \bar{\sigma}_{33}(\boldsymbol{k}) = \frac{\delta^2 k_I^2\bar{r}_{x_1}^2\left(\bar{l}_2(k_p) + \bar{l}_1\right)q_1 + 4k_I^2\bar{l}_1\left[\eta k_I + \bar{l}_2(k_p)\bar{l}_1 + \bar{l}_1^2\right]q_2 + \beta_1 q_3 + \beta_2 q_c}{4\eta k_I\bar{l}_1 L_d(\boldsymbol{k})} \tag{D2ef}$$

and

$$q_1,\ q_2(k_p),\ q_3(k_I),\ q_c(\boldsymbol{k}):\ (14j)$$

$$L_d(\boldsymbol{k}) = \left\{2\eta k_I\bar{l}_2(k_p) + \left[\bar{l}_2(k_p) + \bar{l}_1\right]\left[2\bar{l}_2(k_p)\bar{l}_1 + \delta^2\bar{r}_{x_1}\bar{r}_{x_2}\right]\right\}$$

$$\beta_1(\boldsymbol{k}) = 4\eta k_I\bar{l}_1\left[\eta k_I + \bar{l}_2(k_p)^2 + \bar{l}_2(k_p)\bar{l}_1 + \bar{l}_1^2\right] + 4\bar{l}_2(k_p)\bar{l}_1\left(\bar{l}_2(k_p)^2 + \bar{l}_1^2\right)$$

$$+\ \delta^2\left[4\bar{l}_2(k_p)\bar{l}_1\left(\bar{l}_2(k_p) + \bar{l}_1\right) - 2\eta k_I\bar{l}_1 + \delta^2\left(\bar{l}_2(k_p) + \bar{l}_1\right)\bar{r}_{x_1}\bar{r}_{x_2}\right]\bar{r}_{x_1}\bar{r}_{x_2}$$

$$\beta_2(\boldsymbol{k}) = 4k_I\bar{l}_1\left[2\eta k_I\bar{l}_2(k_p) + 2\bar{l}_2(k_p)^2\bar{l}_1 + 2\bar{l}_2(k_p)\bar{l}_1^2 + \delta^2\left(\bar{l}_2(k_p) + \bar{l}_1\right)\bar{r}_{x_1}\bar{r}_{x_2}\right]$$

### D.2. Marginal state and control PDFs

Knowing the stationary solution of the covariance matrix, it is possible compute the marginal PDFs for concentration ($\mu_{x_1}$), temperature ($\mu_{x_2}$) and integral action ($\mu_{x_3}$) from the approximated steady state PDF (64)

$$\widehat{\mu}_{x_1}(x_1,\boldsymbol{k}) = \frac{1}{\sqrt{2p_n\bar{\sigma}_{11}(\boldsymbol{k})}}\exp\left[-\frac{(x_1 - \bar{x}_1)^2}{2\bar{\sigma}_{11}(\boldsymbol{k})}\right],\ \bar{\sigma}_{11}(\boldsymbol{k}):\ (D2a) \tag{D3a}$$

$$\widehat{\mu}_{x_2}(x_2,\boldsymbol{k}) = \frac{1}{\sqrt{2p_n\bar{\sigma}_{22}(\boldsymbol{k})}}\exp\left[-\frac{(x_2 - \bar{x}_2)^2}{2\bar{\sigma}_{22}(\boldsymbol{k})}\right],\ \bar{\sigma}_{22}(\boldsymbol{k}):\ (D2d) \tag{D3b}$$

$$\widehat{\mu}_{x_3}(x_3,\boldsymbol{k}) = \frac{1}{\sqrt{2p_n\bar{\sigma}_{33}(\boldsymbol{k})}}\exp\left[-\frac{(x_3 - \bar{x}_3)^2}{2\bar{\sigma}_{33}(\boldsymbol{k})}\right],\ \bar{\sigma}_{33}(\boldsymbol{k}):\ (D2f) \tag{D3c}$$

and the unidimensional control $\nu$ PDF can be determined through (20f) by (Papoulis and Pillai, 2002)

$$\widehat{\nu}(u,\boldsymbol{k}) = \frac{1}{2\sqrt{2p_n\bar{\sigma}_u(\boldsymbol{k})}}\exp\left[-\frac{(u-\bar{x}_3)^2}{2\bar{\sigma}_u(\boldsymbol{k})}\right],\ \bar{\sigma}_u(\boldsymbol{k}) = k_p^2\bar{\sigma}_{22}(\boldsymbol{k}) + \bar{\sigma}_{33}(\boldsymbol{k}),\ p_n:\ ``with''\ number \tag{D3d}$$

## References


Abraham, J.R.H., Shaw, C.D., 1992. Dynamics: The Geometry of Behavior. Addison Wesley, New York.

Alvarez, J., Alvarez, J., Suarez, R., 1991. Nonlinear bounded control for a class of continuous agitated tank reactors. Chem. Eng. Sci. 46 (12), 3235–3249. https://doi.org/10.1002/acs.717.

Alvarez, J., Baratti, R., Tronci, S., Grosso, M., Schaum, A., 2018. Global-nonlinear stochastic dynamics of a class of two-state two-parameter non-isothermal continuous stirred tank reactors. J. Proc. Contr. 72, 1–16. https://doi.org/10.1016/j.jprocont.2018.07.012.

Annunziato, M., Borzì, A., Nobile, F., Tempone, R., 2014. On the connection between the Hamilton-Jacobi-bellman and the Fokker-Planck control frameworks. Appl. Math. 5, 2476–2484. https://doi.org/10.4236/am.2014.516239.

Ao, P., 2004. Potential in stochastic differential equations: novel construction. J. Phy. A Math. Gen. 37, L25–L30. https://doi.org/10.1088/0305-4470/37/3/L01.

Aris, R., 1965. Introduction to the Analysis of Chemical Reactor. Prentice-Hall, Englewood Cliffs, New Jersey.

Aris, R., 1999. Mathematical Modeling. A Chemical Engineer's Perspective. Academic Press, London (UK).

Balzano, A., Tronci, S., Baratti, R., 2010. Accurate and efficient solution of distributed dynamical system models. Comput.-Aided Chem. Eng. 28, 421–426. https://doi.org/10.1016/S1570-7946(10)28071-9.

Baratti, R., Tronci, S., Schaum, A., Alvarez, J., 2018. Open and closed-loop stochastic dynamics of a class of nonlinear chemical processes with multiplicative noise. J. Proc. Contr. 21, 108–121. https://doi.org/10.1016/j.jprocont.2018.03.004.

Bashkirtseva, I., Pisarchik, A.N., 2018. Stochastic analysis and control in kinetics of multistable chemical reactor. IFAC-PapersOnLine 51, 545–549. https://doi.org/10.1016/j.ifacol.2018.11.479.

Bashkirtseva, I., 2018. Controlling the stochastic sensitivity in thermochemical systems. Kybernetika 54 (1), 96–109. https://doi.org/10.14736/kyb-2018-1-0096.

Boyce, W.E., Di Prima, R.C., 1967. Elementary Differential Equations and Boundary Value Problems. John Wiley & Sons, New York.

Burr, I.W., 1976. Statistical Quality Control Methods. Routledge, New York.

Doraiswamy, L.K., Kulkarni, B.D., 1986. Relevance of stochastic modeling in chemically reacting systems. Ind. Eng. Chem. Fundam. 25, 511–517. https://doi.org/10.1021/i100024a010.

Franco-de los Reyes, H.A., Schaum, A., Meurer, T., Alvarez, J., 2020. Stabilization of an unstable tubular reactor by nonlinear passive output feedback control. J. Proc. Contr. 93, 83–96. https://doi.org/10.1016/j.jprocont.2020.07.005.

Franco-de los Reyes, H.A., Alvarez, J., 2022. Saturated output-feedback control and state estimation of a class of exothermic tubular reactors. J. Proc. Contr. 93, 78–95. https://doi.org/10.1016/j.jprocont.2022.02.005.

Frank, T.D., 2006. Nonlinear Fokker-Planck Equations: Fundamentals and Applications. Springer Berlin, Heidelberg.

Gardiner, C.W., 1997. Handbook of Stochastic Methods. Springer-Verlag, Germany.

Gavalas, G.R., 1968. Nonlinear Differential Equations of Chemically Reacting Systems. Springer-Verlag, New York.

Gonzalez, P., Alvarez, J., 2005. Combined proportional/integral−inventory control of solution homopolymerization reactors. Ind. Eng. Chem. Res. 44 (18), 7147–7163. https://doi.org/10.1021/ie040207r.

Hirschorn, R.M., 1979. Invertibility nonlinear control systems. SIAM J. Control Optim. 17, 289–297. https://doi.org/10.1137/0317022.

Hirsch, M.W., Smale, S., 1974. Differential Equations, Dynamical Systems and Linear Algebra. Academic Press Inc., London.

Hubbard, J.H., West, B.H., 1995. Differential Equations: A Dynamical Systems Approach. Springer-Verlag, New York.

Jazwinsky, A.H., 1970. Stochastic processes and filtering theory. Academic Press, New York.

Khalil, H., 2002. Nonlinear Systems. Prentice Hall, New Jersey.

Kloeden, P.E., Platen, E., 1992. Numerical Solution of Stochastic Differential Equations. Springer, Berlin.

Krstic, M., Deng, H., 1988. Stabilization of Nonlinear Uncertain Systems. Springer-Verlag, London.

Kwon, C., Ao, P., Thouless, D.J., 2005. Structure of stochastic dynamics near fixed points. PNAS 102, 13029–13033. https://doi.org/10.1073/pnas.0506347102.

Isidori, A., 1999. Nonlinear Control Systems II. Springer-Verlag.

La Salle, J., Lefschetz, S., 1961. Stability by Liapunov's Direct Method with Applications. Academic Press, New York.

LeVeque, R.J., 1992. Numerical Methods for Conservation Laws. ETH Lectures in Mathematics Series. Birkhauser-Verlag.

Lu, Y., Fang, Z., Gao, C., Dochain, D., 2022. Noise-to-state exponentially stabilizing (state, input)-disturbed CSTRs. Automatica 142, 110387. https://doi.org/10.1016/j.automatica.2022.110387.

Mandur, J., Budman, H., 2014. Robust optimization of chemical processes using Bayesian description of parametric uncertainty. J. Proc. Contr. 24, 422–430. https://doi.org/10.1016/j.jprocont.2013.10.004.

Markowich, P.A., Villani, C., 2000. On the trend to equilibrium for the Fokker-Planck equation: an interplay between physics and functional analysis. Matematica Contemporanea 19, 1–29. https://doi.org/10.21711/231766362000/rmc191.

Maxim, A., Copot, D., Copot, C., Ionescu, C.M., 2019. The 5w's for control as part of industry 4.0: Why, what, where, who, and when—a PID and MPC control perspective. Inventions 4 (1), 10. https://doi.org/10.3390/inventions4010010.

McAvoy, T., 2002. Model predictive statistical process control of chemical plants. Ind. Eng. Chem. Res. 41 (25), 6337–6344. https://doi.org/10.1021/ie020067q.

Papoulis, A., Unnikrishna Pillai, S., 2002. Probability, Random Variables, and Stochastic Processes. McGraw-Hill, Europe.

Pell, T.M., Aris, R., 1969. Some problems in chemical reactor analysis with stochastic features. Ind. Eng. Chem. Fundam. 8 (1969), 339–345. https://doi.org/10.1021/i160030a026.

Editor Oates, G.C., 1974. Vector analysis (Ch 3). In: Pearson), C.E. (Ed.), Applied Mathematics. Van Nostrand Reinhold, New York. Editor.

Ratto, M., 1998. A theoretical approach to the analysis of PI-controlled CSTRs with noise. Comp. Chem. Eng. 22 (11), 1581–1593. https://doi.org/10.1016/S0098-1354(98)00232-4.

Ratto, M., Paladino, O., 2000. Analysis of controlled CSTR models with fluctuating parameters and uncertain parameters. Chem. Eng. J. 79, 13–21. https://doi.org/10.1016/S1385-8947(00)00139-X.

Risken, H., 1996. The Fokker-Planck Equation: Methods of Solutions and Applications. Springer-Verlag, Berlin.

Samad, T., 2017. A survey on industry impact and challenges thereof. IEEE Control Syst. Mag. 37 (1), 17–18. https://doi.org/10.1109/MCS.2016.2621438.

Santamaria-Padilla, L., Badillo-Hernandez, U., Alvarez, J., Alvarez-Icaza, L., 2022. On the nonlinear dynamics of biomass throated tubular gasification reactors. Comp. Chem. Eng. 163 (2022), 107828 https://doi.org/10.1016/j.compchemeng.2022.107828.

Schaum, A., Alvarez, J., Lopez-Arenas, T., 2012. Saturated PI control of continuous bioreactors with Haldane kinetics. Chem. Eng. Sci. 68, 520–529. https://doi.org/10.1016/j.ces.2011.10.006.

Schaum, A., Tronci, S., Baratti, R., Alvarez, J., 2021. On the dynamics and robustness of the chemostat with multiplicative noise. IFAC-PapersOnLine 54 (3), 342–347. https://doi.org/10.1016/j.ifacol.2021.08.265.

Sepulchre, R., Janković, M., Kokotović, P., 2012. Constructive Nonlinear Control. Springer Science & Business Media.

Sontag, E.D., 2008. Input to state stability: basic concepts and results. In: Nistri, P., Stefani, G. (Eds.), Nonlinear and Optimal Control Theory, Lecture Notes in Mathematics. Springer, Berlin, Heidelberg, pp. 163–220. https://doi.org/10.1007/978-3-540-77653-6_3.

Tsinias, J., 1998. Stochastic input-to-state stability and applications to global feedback stabilization. Int. J. Control. 71 (5), 907–930. https://doi.org/10.1080/002071798221632.

Uppal, A., Ray, W.H., Poore, B., 1974. On the dynamic behavior of continuous stirred tank reactors. Chem. Eng. Sci. 29 (4), 967–985. https://doi.org/10.1016/0009-2509(74)80089-8.

Vesterinen, T., Ritala, R., 2005. Bioprocesses and other production processes with multi-stability for method testing and analysis. Comput.-Aided Chem. Eng. 29, 421–426. https://doi.org/10.1016/S1570-7946(05)80265-2.

Vidyasagar, M., 1993. Nonlinear Systems Analysis. Prentice-Hall, New York.

Wang, J., Huang, B., Xia, X., Sun, Z., 2006. Funneled landscape leads to robustness of cell networks: yeast cell cycle. PLoS Comp. Bio 2, 1385–1394. https://doi.org/10.1371/journal.pcbi.0020147.

Wu, Z., Zhang, J., Zhang, Z., Albalawi, F., Durand, H., Mahmood, M., Mhaskar, P., Christofides, P.D., 2018a. Economic model predictive control of stochastic nonlinear systems. AIChE J. 64, 3312–3322. https://doi.org/10.1002/aic.16167.

Wu, Z., Durand, H., Christofides, P.D., 2018b. Safeness index-based economic model predictive control of stochastic nonlinear systems. Mathematics 6 (5), 69. https://doi.org/10.3390/math6050069.